ADVANCED SUSTAINABLE SYSTEMS
www.advsustainsys.com

Nanocellulose-Enabled Membranes for Water Purification: Perspectives

Priyanka R. Sharma, Sunil K. Sharma, Tom Lindström, and Benjamin S. Hsiao**

Membrane technology remains the most energy-efficient process for removing contaminants (micrometer-size particles to angstrom-size hydrated ions) from water. However, the current membrane technology, involving relatively expensive synthetic materials, is often nonsustainable for the poorest communities in the society. In this article, perspectives are provided on the emerging nanocellulose-enabled membrane technology based on nanoscale cellulose fibers that can be extracted from almost any biomass. It is conceivable that nanocellulose membranes developed from inexpensive, abundant, and sustainable resources (such as agriculture residues and underutilized biomass waste) can lower the cost of membrane separation, as these membranes offer the ability to remove a range of pollutants in one step, via size exclusion and/or adsorption. The nanocellulose-enabled membrane technology not only may be suitable for tackling global drinking water challenges, but it can also provide a new low-cost platform for various pressure-driven filtration techniques, such as microfiltration, ultrafiltration, nanofiltration, and reverse osmosis. Some relevant parameters that can control the filtration performance of nanocellulose-enabled membranes are comprehensively discussed. A short review of the current state of development for nanocellulose membranes is also provided.

1. Introduction

The demand for low-cost water purification technologies has become a pressing issue because of the rapid population growth in the world. At the turn of the last millennium, we already had over 1 billion people lacking access to safe drinking water and basic sanitation, and nearly 4000 children under the age of 5 dying each day, so the term "clean water crisis" today seems like an understatement.[1] In recent years, significant progress has been made by a joint effort between the World Health Organization (WHO) and United Nations International Children's Emergency Fund (UNICEF), which has led to an increase in the percentage of the global population with clean drinking water from 82% in 2000 to 91% in 2015.[2] Although the project was a major success, especially in such a short time frame, it cannot be overlooked that as of 2015, close to 675 million people still lack access to safe drinking water and 2.4 billion people are still without proper sanitation. Furthermore, the WHO/UNICEF initiative fell short when it came to the least developed countries, as well as in rural areas, where an astounding 16% of the global rural population does not have access to safe drinking water, and a higher percentage lacks sanitation.[2] What is particularly alarming is that in rural regions within Africa, innumerable cases of waterborne diseases, such as cholera, diarrhea, guinea worm, and various parasites, threaten the lives of many communities on a daily basis.[3] In total, the variety of viruses, bacteria, and parasites that lead to diarrheal conditions are the cause of between 2 and 2.5 million deaths per year on the global stage.[3] Therefore, it is essential to develop lower-cost and more sustainable water purification technologies that are not available today. In this article, we focus on one possible pathway to tackle the above challenges using abundant, renewable, and inexpensive natural biomass as a sustainable source to extract nanoscale materials (nanocellulose) for water purification. In a recent review, nanocellulose has been shown to be a valuable sorptive material, comparable with activated carbon or carbon nanomaterial, for removing contaminants.[4] In this article, we provide the current state-of-the-art technologies as well as perspectives regarding the use of nanocellulose as a valuable building block for fabrication of low-cost water filtration membranes. Although nanocellulose-enabled membrane technologies are only in the initial stage of development, we believe that they will grow rapidly in the future. We also note that these technologies may take advantage of existing paper/packaging processes, although the final products (stable membranes with controllable pore size and porosity) for water filtration will have very different requirements and considerations, which are also discussed here.

1.1. Structural Perspectives of Conventional Membranes

Pressure-driven membrane filtration technologies, from microfiltration (MF) for separating large particles from water to reverse osmosis (RO) for separating salt ions from

Dr. P. R. Sharma, Dr. S. K. Sharma, Prof. T. Lindström, Prof. B. S. Hsiao
Department of Chemistry
Stony Brook University
Stony Brook, NY 11794-3400, USA
E-mail: toml@kth.se; benjamin.hsiao@stonybrook.edu
Prof. T. Lindström
KTH Royal Institute of Technology
Stockholm 100 44, Sweden
The ORCID identification number(s) for the author(s) of this article can be found under https://doi.org/10.1002/adsu.201900114.

DOI: 10.1002/adsu.201900114

water, remain one of the most energy-efficient pathways for water purification.[5] The principle of these separations is straightforward. Typically, contaminants (e.g., molecules or metal ions) move naturally from regions of high concentration to low concentration, whereupon applying external pressure, contaminants then flow from regions of low concentration to high concentration; this process can purify water. The classification of pressure-driven membrane filtration techniques, and their pore size and pressure relationship, are illustrated in **Figure 1**. Generally speaking, membranes with smaller pore size will require higher pressure to operate. To operate a filtration system with high pressure, one needs not only a reliable supply of energy (e.g., electrical and mechanical), but also the use of robust equipment (e.g., a pressure pump). The combined requirements are often beyond the reach of the poorest communities that need low-cost safe drinking water the most.

However, there is one pressure system, driven by gravity, that can have very low cost and is easy to maintain, making it particularly suited for poor communities living off the grid. The corresponding filtration operation that can be driven by gravity is microfiltration (Figure 1). This is because gravity-driven MF membranes possess the lowest mean pore size of ≈0.2 µm, which is sufficient to remove most common harmful bacteria (e.g., *Escherichia coli*, *Hepatitis A, Salmonella,* and *Cryptosporidium*) from water.[6] Figure 1 illustrates the relationship between the pore size and pressure for different types of pressure-driven membranes. The conventional membrane can be divided into two classes. The first class of membranes (MF and ultrafiltration (UF)) has a mean pore size greater than 1 nm and is often termed porous membranes. The predominant removal mechanism in these membranes is size exclusion, where the filtration process can achieve high efficiency that is mostly independent of the pressure and concentration of contaminated water.[7–10] The second class of membranes (nanofiltration (NF) and RO) does not have visible pores, and their theoretical pore size is equal to or less than 1 nm. These membranes are often viewed as nonporous membranes. The predominant removal mechanism for these membranes is through differences in the solubility or diffusivity of contaminant and water molecules, where the process is dependent on pressure and solute concentration.[11]

For water filtration, most porous polymeric membranes (MF to UF), including hollow fibers, are manufactured by the phase inversion method.[12,13] The resulting structure, whether used directly in the barrier layer or indirectly in the supporting layer (for NF and RO), has some intrinsic limitations. These limitations include low flux (thus high energy cost) and high fouling tendency resulting from the asymmetric pore structure and distribution across the membrane thickness.[13] The typical schematic diagram of a thin film composite (TFC) membrane for water is illustrated in **Figure 2**.[14] Such a membrane structure, containing three layered components, has remained unchanged since its inception in the 1970s. The three layers include 1) a nonwoven substrate (based on micrometer-size fibers) that can be considered a low-end MF membrane, 2) a porous layer (made by the phase inversion method) that can be used directly as an UF membrane, and 3) a densely cross-linked barrier layer (fabricated by the interfacial polymerization method) that renders the membrane useful for NF and RO applications. The requirement of each component layer is different: the nonwoven substrate layer needs to be strong to provide overall mechanical strength, and it usually has the highest porosity (60–70%); the middle porous layer must have a uniform pore distribution on the layer surface (as the

Priyanka R. Sharma received her Ph.D. in 2014 from CSIR-National Chemical Laboratory. In 2015, she joined Stony Brook University as a postdoctoral research associate with Prof. Benjamin Hsiao. Currently, she is working as a research scientist in the Department of Chemistry, Stony Brook University. Her research interests are on the development of novel sustainable materials for water purification, environmental, and energy-related applications, as well as structural characterization of nanocellulose by advanced microscopy and synchrotron techniques.

Tom Lindström has wide experience in most sectors of the Forest Products Industry. This experience encompasses academic, institutional, and industrial activities. Lindström's scientific and technical interests are the physical and surface science of cellulosic fibers and wood-based materials and Physio-chemical swelling behavior of cellulose/lignin gels; a long focus has been on various paper chemistries. During the past few years, his focus has been on the manufacture and upscaling of nanocellulosic materials and various industrial applications of these materials.

Benjamin S. Hsiao is a Distinguished Professor in Chemistry at Stony Brook University. He is the Founding Director of the Center for Integrated Electric Energy Systems with the mission of developing advanced technologies to enhance the nexus of food, energy, and water. Hsiao's current research interests are focused on the development of sustainable nanomaterials from underutilized biomass for water purification.

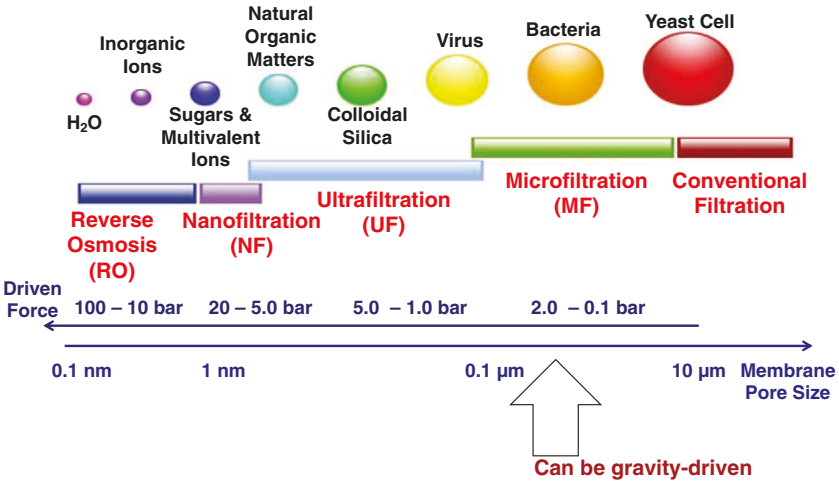

Figure 1. Classification of pressure-driven membrane filtration, and their pore size and pressure relationship.

supporting layer or the barrier layer), and it has a relatively low porosity (25–50%); the top barrier layer (typically an interfacially polymerized cross-linked polyamide matrix) has the smallest pore size distribution as well as the lowest porosity.

1.2. New Advances in Nanofiber Membranes

From a structural perspective regarding the conventional filtration membrane design (Figure 2), it seems that to reach a smaller pore size, one has to sacrifice porosity, based on the typical manufacturing methods. However, this limitation can be avoided, to some extent, using nanofiber technology. An exemplary argument is illustrated in **Figure 3**, where the schematic diagram of a nonwoven structure containing 80% porosity with different fiber diameters is shown. When the fiber diameter is reduced, the effective mean pore size is also reduced, while the porosity maintains unchanged. Generally, the mean pore size is directly proportional to the fiber diameter in the nonwoven fiber membrane, where as the fiber diameter decreases, the effective pore size also decreases.

Based on the above concept, our group at Stony Brook has developed a new class of nanofiber membranes for water purification. The major innovation of this nanofiber membrane technology is that membranes made of nanofiber materials (synthetic and natural) in the nonwoven format because of the high porosity (up to 80%) can drastically improve the flux capacity (e.g., often with a flux increase of many times), thereby permitting lower operating pressures but retaining the resistance to fouling. Better flux means less time to filter the same amount of water, which in turn decreases energy consumption and increases cost efficiency. Better resistance to fouling refers to the ability to avoid clogging of the membrane pores by foreign matter, such as oil, detergents, biomacromolecules, and salts, which can accumulate during the purification process.

An exemplary three-layered nanofiber membrane with UF or NF performance is shown in **Figure 4**. This new format also contains 1) a nonwoven substrate with micrometer-size fibers to provide mechanical strength; 2) a nonwoven mid-layer scaffold with sub-micrometer-size fibers (100–300 nm, made by the electrospinning method) that can be used directly as a high-end or low-pore-size MF membrane; and 3) a nonwoven top barrier layer with nanometer-size fibers (2–5 nm cellulose nanofibers extracted from biomass) that can be used directly as a UF membrane. Nanofiber membranes are good alternatives that can surpass conventional membranes. This is because all three nonwoven layers have relatively high porosity (typically around 80%), fully interconnected open pore structures, and controllable pore size distribution from micrometers to nanometers, thus providing high permeability for water filtration.

Additionally, nanofiber membranes offer some extra advantages over conventional membranes because of their high surface-to-volume ratio (especially the top nanocellulose barrier layer) and easy surface modification schemes. For example, the abundant functional groups on nanocellulose (e.g., the hydroxyl and carboxylate groups on cellulose nanofibers) can provide excellent adsorption sites to remove many organic and inorganic contaminants.[17,18] Thus, the combined high-flux filtration and high adsorption performance in an MF membrane with the interpenetrating fibrous composite format, based on an electrospun nanofibrous scaffold infused with finer cellulose nanofibrous webs, has been shown to be capable of removing common bacteria, viruses, and toxic metal ions simultaneously using gravity-driven operation.[16,17,19–21] It is thought that the electrospun nanofibers can be replaced by nanoscale cellulose fibers, where the MF membrane system, based entirely on

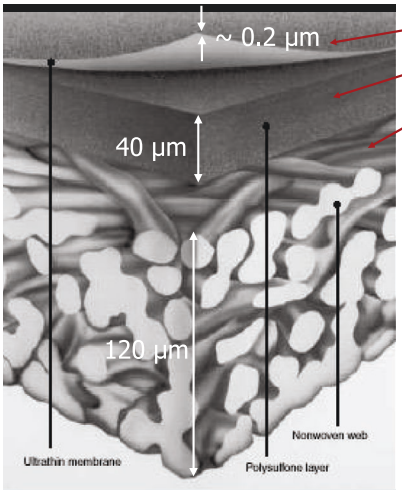

RO/NF layer
UF layer
Non-woven MF support

Size exclusion range
RO (Reverse Osmosis): < 1 nm
NF (Nano-Filtration): 1 – 10 nm
UF (Ultra-Filtration): 10 – 100 nm
MF (Micro-Filtration): 0.1 – 50 ∝m
Aqueous salts: 0.3 – 1.2 nm
Pesticides, herbicides: 0.7 – 1.2 nm
Virus: 10 – 100 nm
Bacterial: 200 nm – 30 ∝m

	Pressure (psi)	Flux (l/m²h)
UF	15 – 150	3 – 100 (pure water)
NF	70 - 400	0.22 – 0.66 (e.g. 2000 ppm $MgSO_4$)
RO	70 – 400 (Brackish Water) 600 – 1200 (Seawater)	0.03 – 0.40 (Brackish water : 1000 – 5000 ppm salts; Seawater : 35,000 ppm of salts)

Figure 2. Conventional water filtration thin film composite membrane structure (since the 1970s).[14]

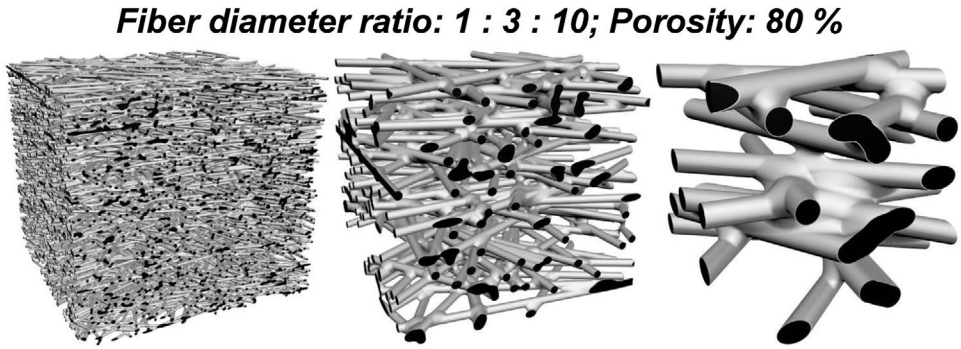

Figure 3. The relationship between fiber diameter and pore size in nonwoven membranes. Reproduced with permission.[15] Copyright 2012, American Chemical Society.

cellulosic components, will be an ideal inexpensive and sustainable platform that can be utilized to deal with the drinking water crisis in the remote regions of developing countries, where material and electrical energy resources are very limited.

1.3. Contemporary Drinking Water Technologies for Off-Grid Communities

Currently, there are several water purification technologies, although not all include the use of membranes, that have been designed and demonstrated to improve the access of safe drinking water for off-grid communities or remote regions without water infrastructure. These technologies are summarized in **Figure 5** (e.g., based on the inhabitat website,[22,23]) and they are briefly described below. Unfortunately, the cost of these technologies to purify drinking water is often too high to be afforded by the poorest off-grid communities.

1.3.1. LifeStraw

LifeStraw is a cigar-shaped plastic tube having a length of 31 cm and diameter of 3 cm (Figure 5A). It is composed of hollow fibers (MF-grade) that can filter particles up to 0.2 µm using only suction pressure. This system can remove up to 98.9% of bacteria and protozoans (e.g., *Giardia lamblia* and *Cryptosporidium*) that are commonly responsible for waterborne diseases in human beings. Each LifeStraw can filter 1000 L of water, which is sufficient for one year for each person. Because of their easy accessibility and excellent results concerning the removal of bacteria and protozoans, they have been distributed

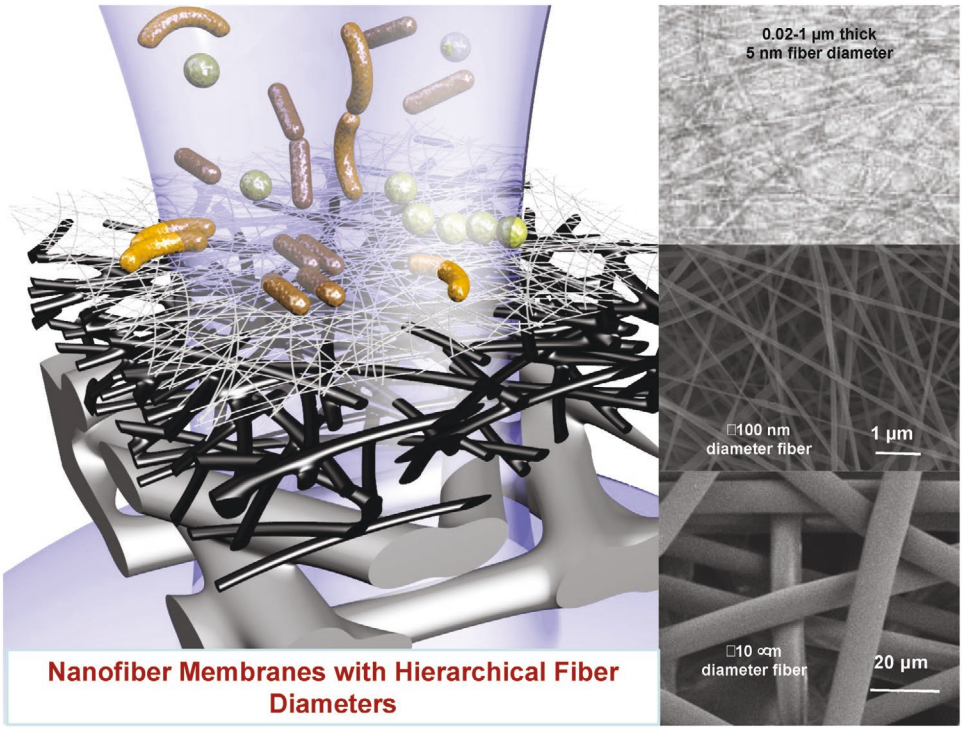

Figure 4. Three-layered nanofiber membranes with hierarchical fiber diameters from micrometers to nanometers. Reproduced with permission.[16] Copyright 2011, American Chemical Society.

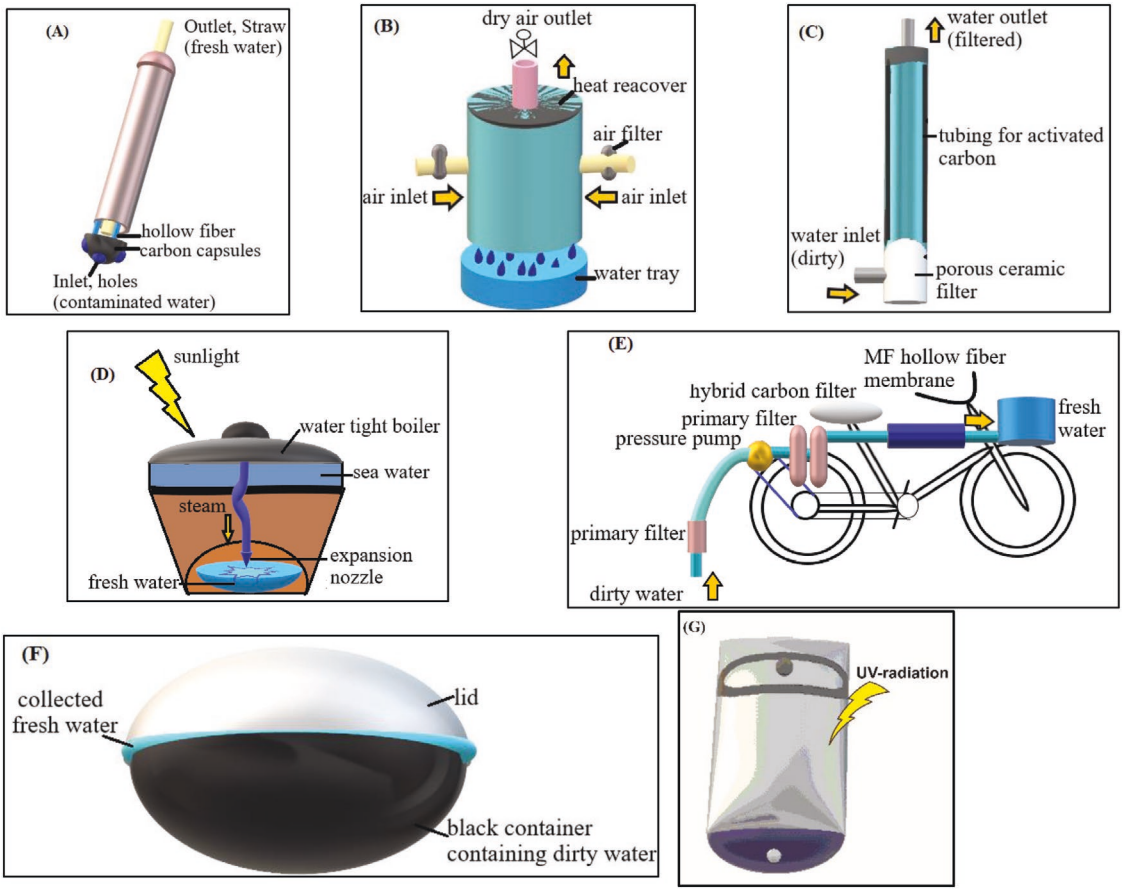

Figure 5. Some of the current state-of-the-art water purification technologies established for off-grid communities: A) LifeStraw, B) EcoloBlue, C) ceramic filters, D) Eliodomestico solar still, E) CycloClean, F) Hamster ball-shaped solar ball, and G) Life Sack.

during several natural disasters, including the Haiti earthquake in 2010[24] and Ecuador earthquakes[25] in 2016. Unfortunately, LifeStraw is not effective for removing viruses, metal ions, chemicals, or salts.

1.3.2. EcoloBlue's Atmospheric Water Generator (AWG)

EcoloBlue is a technology that draws water from the atmosphere (Figure 5B). A small office/home model has the capacity to generate seven gallons of water per day. The system is composed of a stainless-steel tank with a filtration and condensation unit, which functions well at above 30% humidity. However, the system is too expensive ($1350 for a small unit) for most people in off-grid communities. The success story of EcoloBlue's AWG started in California during the drought in 2014.[26] Because of its effective utilization during the California crisis, the State of California has approved this technology for use as an alternative water source.

1.3.3. Ceramic Water Filters

Water filters made of ceramics can effectively remove bacteria, protozoa, and microbial cysts from drinking water. However, they are ineffective for removal of chemicals, metal ions, and viruses. The major advantages of ceramic water filters are their long usage life and ease of cleaning. However, the major limitation is the relatively high cost. Many water-stressed developing countries, such as Nigeria, Ghana, Kenya, India, Vietnam, and Sri Lanka, have initiated ceramic water filter industries in the form of clay pot filters to provide high-quality potable water.[27] Figure 5C illustrates a water filtration apparatus designed for an off-grid community, based on the combined use of porous ceramic filters and active carbon (which can also adsorb the pungent smell caused by chemicals like chlorine).

1.3.4. Eliodomestico Solar Still

This is a simple and relatively inexpensive device that can covert seawater into drinkable water using only sunlight (Figure 5D), and it has been successfully tested in some arid coastal regions around the world. The device consists of a vessel (which can be made of clay) with a lid and a tube. In the presence of sunlight, steam is generated in the closed vessel and then passed to the bottom of a container through an expansion nozzle to generate portable water. This is a cost-effective way to purify water, as it does not require electricity, moving parts, or filters. However, the throughput is generally

low. This project won a Core77 design award for social impact. The ultimate objective of this project was to deliver the idea of Eliodomestico[28] to local craftsmen all over the world, so that people in need can effortlessly obtain access to clean drinking water at low cost.

1.3.5. Water Purifying Bicycle (Cycloclean)

This is a bicycle-powered water purification system that can filter water using pedal power (Figure 5E). The system is composed of a sucking pump, a primary filter containing activated carbon, a secondary filter based on an MF membrane, and a reservoir. The Cycloclean can purify 3 tons of water in 10 h, and the lifetime of the filter is ≈2 years.[29] The Cycloclean design was first demonstrated by the Japanese government and exhibited at a unit cost of $6600. Recently, Nippon Basic announced that they are planning to launch these bicycles in Bangladesh at a more affordable price.

1.3.6. Hamster Ball-Shaped Solarball

The spherical Solarball (Figure 5F) absorbs sunlight and causes the evaporation of dirty water, leaving behind contaminants. The collected evaporated water is suitable for drinking. This unit has been demonstrated successfully at a small scale, but it generates less than a gallon per day of drinking water.[30]

1.3.7. Life Sack

Life Sack is a multiple-purpose transparent sack (Figure 5G) that can purify water as well as be used for storage (e.g., grain). The system uses the solar water disinfection process (SODIS) to filter contaminated water. In brief, the UV-A radiation from sunlight and the thermal treatment of the bag work collectively to disinfect the water by killing deadly microorganisms and bacteria,[31] where the treated water will pass through a UF filter to become drinkable water.

It is clear that the above off-grid technologies are primarily suitable for small-scale production of portable water, which can be utilized for individual or single-family consumption. To increase the volume of portable water generation, the technology is often reduced to the removal of particles greater than 0.2 μm, such as bacteria, microbes, and protozoa.[22] Because a large portion of the population (16%)[2] in underdeveloped countries is off grid and most in need of low-cost safe drinking water, a new decentralized technology is necessary to tackle this challenge. Here, we argue that nanostructured cellulose-enabled technologies (at the micro or nanoscale) represent a promising pathway to develop "decentralized" large-scale processes to alleviate the global drinking water crisis.

1.4. Nanocellulose: An Emerging New Material for Water Purification

The methods of adsorption, absorption, flocculation, and coagulation have been adopted in many water purification processes because they are able to remove contaminants such as microbes and chemicals (metal ions, dyes, and organic molecules) at relatively low cost.[32] Cellulose and its derivatives have long been recognized as a class of sustainable and effective material suitable for various adsorption, absorption, flocculation, and coagulation treatments.[33] For example, a quick search of SCIFINDER on the topic of cellulose together with adsorption, absorption, coagulation, and flocculation indicates that nearly 1200 articles (including patents and research papers) were published between 2000 and 2017 (**Figure 6**A).

Among the cellulose family, cellulose nanomaterials (CNs) or nanocellulose has been recognized as a particularly promising water purification material. Nanocellulose or CNs represents all nanoforms of cellulosic materials, including cellulose nanofibers (CNFs), nanocrystalline cellulose, cellulose nanocrystals (CNCs), cellulose nanofibrils, and cellulose

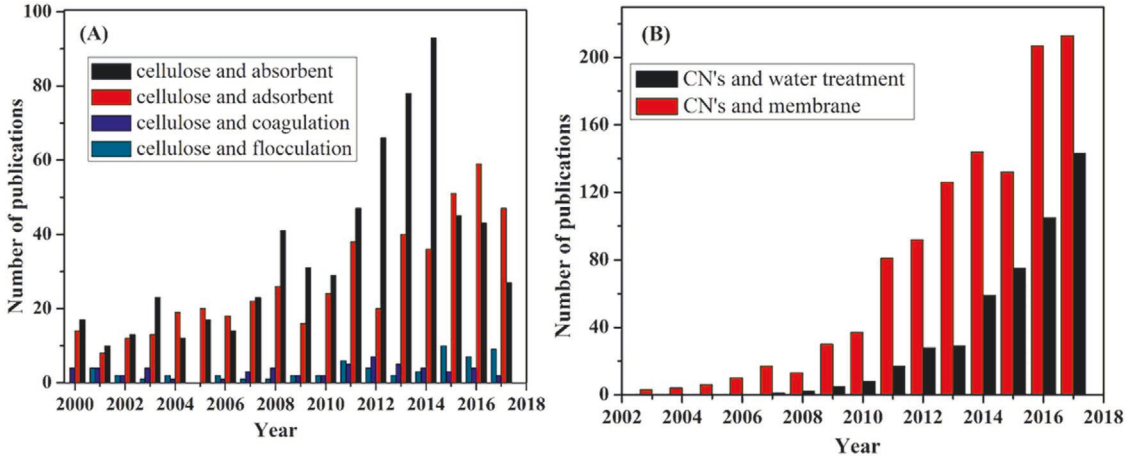

Figure 6. A) Graph presenting number of publications on the topic of cellulose linked to absorption, adsorption, coagulation, and flocculation; B) graph presenting number of publications on the topic of cellulose nanomaterials (CNs) and water treatment, as well as CNs and membrane (CNs represents all nanoforms of cellulose, including cellulose nanofibers, nanocrystalline cellulose, cellulose nanocrystals, cellulose nanofibrils, and cellulose nanowhiskers).

nanowhiskers, where CNFs and CNCs have been recognized as the two most popular sub-families. CNFs usually have a larger aspect ratio, smaller cross-sectional dimensions, and lower crystallinity than CNCs. A quick search of SCIFINDER on the topic of CNs/water treatment and CNs/membrane yields some interesting observations (Figure 6B). Although both combined subjects show a rapid increase (papers and patents and patent publications), the topic of CNs/membrane is increasing more quickly than CNs/water treatment. This is because the subject of CNs/membrane consists of varying applications other than water treatment. Some example applications are membranes for separation of byproducts,[34,35] thermoresponsive membranes,[36] DNA extraction membranes,[37] hemodialysis membranes,[38] antibacterial membranes,[39,40] catalytic membranes,[41] and hydrogen-permeable membranes.[42] Applications related to water treatments include fluoride removal membranes,[43] substrates to remove humic acid,[44] separation of xenotropic murine leukemia virus,[10] and separation of metal ions and dyes.[43,45–47] It may be the case that, because of the high cost of CNs production, a good portion of the CNs/membrane studies are leaning toward high-valued separations.

Clearly, the topic of CNs/water treatment is also seeing a rapid increase (Figure 6B). However, this topic also involves the use of CNs as adsorption, absorption, flocculation, and coagulation media, where their performances have been proven to rival and even exceed those of carbon nanomaterials (including activated carbon, carbon nanotubes, and carbon nanofibers). Some excellent reviews dealing with this topic have recently been published;[4,47–49] they are not discussed here. Instead, we focus on the topic of CNs/membrane/water treatment, i.e., the development and applications of nanocellulose membranes for water purification. The article includes a short review of recent success concerning nanocellulose-enabled membranes for MF and UF operations, where significant energy-saving benefits can be realized. This article also covers the challenges and solutions associated with the low-cost production of nanocellulose membranes on a large scale, where key processing and manufacturing (defibrillation) parameters in pretreatment and surface modification steps for facilitating the defibrillation of cellulose fibers are discussed. Finally, using recent advances in synthetic nanofiber membranes (Section 1.1) as a reference, we also discuss the use of natural nanocellulose, which can replace synthetic nanofibers for more demanding water purification processes, such as RO, forward osmosis (FO), and membrane distillation (MD).

2. Cellulose and Nanocellulose

Cellulose is the most abundant natural polymer on earth. Its annual production is on the order of 7.5×10^{10} tons,[50] which corresponds to an annual carbon production of 30×10^9 tons. This carbon production can be compared with the total carbon emissions from fossil fuel consumption, which amounts to 9×10^9 tons.[51] Cellulose is produced by higher plants; a wide range of bacteria, algae, and fungi; and certain animals, such as tunicates.[52] Both wooden and nonwooden plant fibers can be used to extract nanocellulose. In **Table 1**, the chemical composition of wood-based fibers and various plant fibers have been compiled. The general consensus is that nonwooden plants usually have a lower lignin content than wooden plants, which makes the nonwooden plant fibers easier to delignify, thus facilitating the nanocellulose extraction process. The current chemistries for nanocellulose extraction have primarily been developed to deal with wooden plants. For lower-value nonwooden plants, such as agricultural residues, the major focus today is the production of biofuels.[53] We argue that as the logistics of collection, transportation, and decortication for biofuel production are being worked out to deal with agricultural residues, the exploration of new and simple chemistries that can extract nanocellulose from nonwooden plants[54] in a more cost-effective manner than the existing approaches using wooden plants can definitely enable us to develop low-cost nanocellulose processes to upcycle vastly underutilized nonwooden biomass, especially for water purification. Agricultural residues are often utilized as a burning source for waste removal or energy generation, which causes undesired air pollution.[55]

Table 1. Compilation of the content of cellulose, hemicellulose, and lignin in various biomass sources.[56]

Biomass waste	Cellulose	Hemicellulose	Lignin
Softwood	45–50	18–35	23–35
Hardwood	40–50	24–40	18–25
Wheat straw	35–39	22–30	12–16
Rice straw	29.2–34.7	23–25.9	17–19
Corn stover	35.1–39.5	20.7–24.6	11.0–19.1
Corn cob	32.3–45.6	39.8	6.7–13.9
Cotton stalk	31	11	30
Barley straw	36–43	24–33	6.3–9.8
Sorghum straw	32–35	24–27	15–21
Nut-shell	25–30	22–28	30–40
Rice husk	28.7–35.6	11.9–29.3	15.4–20
Bagasse	25–45	28–32	15–25
Agave leaves	64–70	22–28	5–7
Switchgrass	30–35	20–25	15–20

During recent decades, there has been a rapid growth in research and commercial interests directed toward the development of nanocellulose materials. The production methods can be divided into two paths: the bottom-up approach, which involves the use of bacteria to convert sugars into nanocellulose (bacterial nanocellulose); and the top-down approach, which involves the use of various enzymatic/chemical/mechanical processes to break down fibers to their elementary microfibrillar or aggregate forms. In typical vascular plants, cellulose is synthesized in the plasma membrane by the rosette terminal complexes, containing synthase enzymes that produce individual polymer chains. Such a synthesis is a two-step process, where the resulting elementary microfibrils represent the aggregation of cellulose chains produced from one rosette terminal complex (**Figure 7**, where 18-chain microfibrils are shown). The cross-sectional dimensions of the elementary microfibril are usually in the range of 2–4 nm; depending on the assembly of the chain, the length of the microfibril can be on the order of micrometers.[57] The cross-sectional dimensions

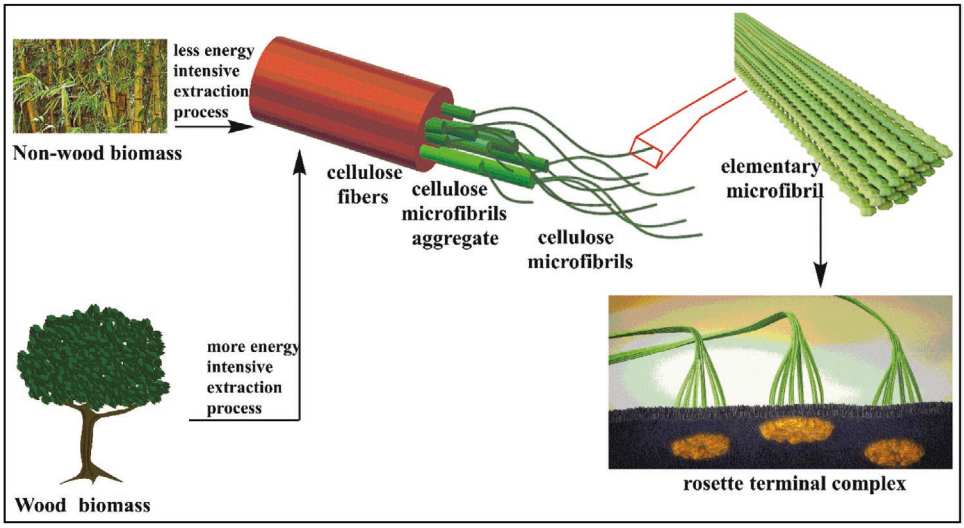

Figure 7. The hierarchical structure of cellulose in biomass.

of the microfibril aggregate are typically in the range of 2–30 nm, depending on the defibrillation conditions.[58]

Conventionally, nanocellulose can be divided into three categories: microfibrillar cellulose (MFC)/nanofibrillar cellulose (NFC), nanocrystalline cellulose (NCC), and bacterial nanocellulose (BNC), where several comprehensive reviews are available to discuss this subject.[65] There are a few other forms of nanocellulose, such as spherical nanoparticles[61] and nanoribbons,[62,63] that cannot be included in the above categories. **Table 2** illustrates the three categories of nanocellulose, as well as their common synonyms, typical sources, and average dimensions.

However, with recent manufacturing advancements for processing nanocellulose, the final products often fall into two categories: cellulose nanofibrils (CNFs) and cellulose nanocrystals (CNCs). Typically, CNCs are produced by the acid hydrolysis route,[59,62,64,65] resulting in needle-like cellulose crystals with higher crystallinity (above 60%), shorter length (several hundred nanometers), and a lower degree of polymerization than CNFs.[64] CNFs are usually produced by chemical modification of cellulose surfaces, such as TEMPO (2,2,6,6,-tetramethylpiperidine-1-oxyl radical) oxidation[66]or carboxymethylation,[67] to introduce a negatively charged surface that can facilitate the defibrillation process. As a result, CNFs possess lower crystallinity (≈30%), smaller cross-sectional dimensions (2–10 nm), longer length (several micrometers), and a higher degree of polymerization. However, both CNCs and CNFs are mechanically strong,[59] chemically stable, and hydrophilic,[68] making them quite suitable for use in various water treatment technologies. From the perspective of membrane fabrication, CNFs are a more suitable building material because of their higher aspect ratio, larger interfibrillar connectivity (resulting from fiber entanglement), smaller cross-sectional dimensions (thus smaller membrane pore size), and easier functionalization. In contrast, CNCs seem to be more suitable for use as a functional nanofiller material. As a result, we focus primarily on the production of CNFs in this article.

3. Nanocellulose Extraction

3.1. Conventional Extraction Procedures from Wood Biomass

Nanocellulose (e.g., CNFs and CNCs) can be extracted from any cellulose-containing biomass. Currently, commercially available CNFs/CNCs are typically produced from wood-based

Table 2. Three common categories of nanocellulose, as well as their synonyms, typical sources, and sizes.

Type of nanocellulose	Synonyms	Typical sources	Average sizes
Microfibrillated cellulose (MFC) or nanofibrillar cellulose (NFC)	Cellulose nanofibrils, cellulose microfibrils, and nanofibrillated cellulose	Wood, sugar beet, potato tuber, hemp, and flax	Diameter: 3–60 nm; Length: several micrometers
Nanocrystalline cellulose (NCC)	Cellulose nanocrystals, cellulose crystallites, cellulose whiskers, rod-like cellulose, and cellulose microcrystals	Wood, cotton, hemp, flax, wheat straw, mulberry bark, ramie, and tunicin	Diameter: 3–60 nm; Length: 100–250 nm
Bacterial nanocellulose (BNC)	Bacterial cellulose, microbial cellulose, and biocellulose	Low-molecular-weight sugars and alcohols	Diameter: 20–100 nm; Length: several micrometers

pulp fibers prepared first by delignification, followed by bleaching.

3.1.1. Wood Pulping

Pulping is a process (also called the delignification process) for conversion of wood into wood pulp, which consists of almost pure cellulose fibers. Kraft pulping is the most popular pulping process, where wood chips are pulped using a mixture of sodium sulfide and sodium hydroxide. After pulping, fibers are bleached by chlorine dioxide oxygen, ozone peroxide, or alkaline extractions. An alternate pulping process is sulfite pulping. In this process, wood chips are first digested in the presence of sulfite or bisulfite liquors. This process is a less favorable method. It is also possible to extract cellulose fibers directly from wood using mechanical or (chemi)mechanical pulping processes. As the cohesion forces of the cell walls caused by lignin are very strong, very high energy consumption is usually necessary using the purely mechanical route.

3.1.2. Mechanical Defibrillation

To extract CNFs, proper mechanical equipment for defibrillation/delamination of cellulose fibers is necessary.[69] More conventional defibrillation methods include homogenization,[70] refining,[71] and microfluidization,[72,73] where less conventional methods include extrusion,[74] steam explosion,[75] ball milling,[76] ultrasonification,[77] aqueous counter-collision (AQQ),[78] and high-speed blending.[79] The original inventors[60,70] of "microfibrillar cellulose" used high-pressure homogenizers to defibrillate cellulose fibers, without any chemical pretreatment. These inventors found that the energy consumption of the process was very high and that there was extensive clogging of the homogenizers, particularly when the pulp consistency increased. The term "clogging" is related to the extent to which cellulose fibers are susceptible to flocculation and hence clog the interaction chambers during defibrillation. The above problems have been overcome by the development of several innovative chemical pretreatments, which enable the commercial exploitation of CNFs/CNCs manufacturing. Below, we will mostly discuss the extraction of CNFs, which is more relevant as a building material for membranes.

3.1.3. Chemical Pretreatment to Facilitate Defibrillation

Chemical pretreatments to facilitate the defibrillation of cellulose fibers into CNFs can be categorized into two classes: 1) electrostatically induced swelling by introduction of charged groups onto cellulose chains, which can be accomplished in either the pulping or bleaching step or by subjecting cellulose fibers to oxidative treatment, such as TEMPO-mediated oxidation;[66] and 2) mild acid or enzymatic hydrolysis of cellulose fibers.[72] Both processes can decrease the cell wall cohesion and hence reduce energy consumption during defibrillation of cellulose fibers. It is known that the cell walls in pulped wood fibers have naturally occurring charged groups, such as carboxyl groups, formed by ester cleavage of hemicellulose molecules during pulping or by disproportionation reactions in the residual lignin molecules. These charged groups can facilitate the swelling and decrease the cell wall cohesion in cellulose fibers. The charge content can be significantly increased through a number of oxidation and chemical modification procedures, including carboxylation via periodate-chlorite oxidation,[80] sulfonation,[81] carboxymethylation,[67] TEMPO-oxidation,[66] cationization,[82] nitro-oxidation,[83,84,85] and phosphorylation.[86] It has been reported that the original charge content in wood pulp fibers is in the range of 30–250 μeg g^{-1}, where the charge content can be increased to 300–2000 μeg g^{-1} after chemical pretreatment.[87] The high charge content can drastically decrease the energy consumption during defibrillation of cellulose fibers. **Figure 8** illustrates the effect of charge content on the estimated energy consumption for disintegration of cellulose fibers into nanofibers,[89] where energy savings of orders of magnitude can be obtained with a suitable pretreatment procedure.

The charge content on cellulose fibers also has a significant effect on the flocculation of fibers by affecting the friction through electrostatic double-layer repulsion. Kerekes and co-workers developed the "crowding factor" concept, defined as N fibers in a conceived volume according to Equation (1), to describe the behavior of fiber flocculation[88]

$$N = 5C_m L^2/\omega \quad (1)$$

where C_m is the mass consistency, L is the fiber length, and ω is the fiber coarseness. This equation is intuitively simple to grasp, as long fibers with higher consistency and lower ω would increase the tendency to flocculate. The friction between the fibers is, however, not included in this concept, the impact of which was later realized by Kerekes. It has also been shown that the rheology of pulp suspensions are strongly affected by charge interactions.[90] It is clear that these interactions are critical for clogging interactions, which can be reduced by a high charge content during fiber defibrillation.

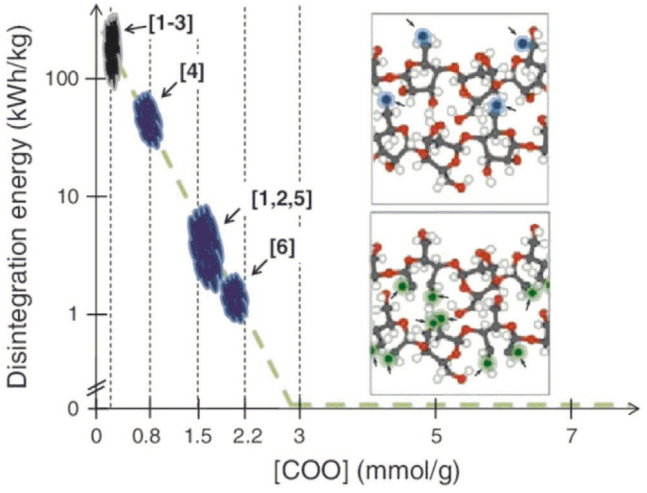

Figure 8. The effect of charge content on the estimated energy consumption for defibrillation of cellulose fibers into nanofibers. Reproduced with permission.[89] Copyright 2012, Springer Nature.

3.2. CNF Extraction from Nonwood Biomass

As indicated earlier, nonwooden plants usually have a lower lignin content than do wooden plants (Table 1), which makes the extraction of CNFs from nonwood biomass much easier, sometimes by bypassing the pulping (delignification) and pretreatment steps. For example, untreated *Triodia pungens* spinifex (an Australian grass) can be readily used to produce high-aspect-ratio CNFs with very small widths (2–10 nm) after mild pulping using sodium hydroxide and just one pass through a high-pressure homogenizer at relatively low pressure.[91]

3.2.1. Nitro-Oxidation Method

Recently, a simple nitro-oxidation method has been developed in our laboratory to prepare CNFs directly from raw biomass (jute, spinifex grass, and bamboo) using only nitric acid–sodium nitrite mixtures.[85,92] In this method, the lignin component is depolymerized into soluble benzoquinone products by the presence of nitrogen oxide species (produced by the reaction of nitric acid and sodium nitrite), and the hemicellulose component is broken down into xylose and other by-products by nitric acid.[93] In addition, the generation of nitroxonium ions can selectively oxidize the primary hydroxyl groups of the anhydroglucose units of cellulose to carboxyl groups. As a result, the nitro-oxidation method significantly reduces the need for multiple chemicals and the consumption of electric energy and water for producing CNFs. A process diagram comparing the conventional TEMPO-oxidation method and the nitric-oxidation method to extract CNFs from nonwooden plants is illustrated in **Figure 9**. In addition, the effluent (spent liquor) from this method could be neutralized using a base to produce nitrogen-rich salts as plant fertilizers to avoid expensive recovery operations. The idea of using the spent liquor as a fertilizer was investigated by Brink.[94,95]

However, despite the promising potential of the nitro-oxidation process, it has not yet been optimized or proven applicable at the industrial scale. This is because nitric acid is a strong acid and a potent oxidant that can easily break down carbon–carbon bonds, resulting in cellulose with a low degree of polymerization. Historically, there has been a large amount of work devoted to nitric acid pulping, and there are also several reviews available on this topic.[96] The specificity of the oxidation can, however, be enhanced by the use of nitrogen dioxide instead of nitric acid.[97] It is conceivable that the gas-phase oxidation approach involving nitrogen dioxide (NO_2) may greatly simplify the water-consuming and postoxidation rinsing steps and leave fewer residuals on the treated cellulose.

3.3. Characterization of CNFs

CNFs can be characterized by varying techniques with respect to their structure and morphology. These techniques include transmission electron microscopy (TEM), scanning electron microscopy (SEM), field-emission scanning electron microscopy (FE-SEM), atomic force microscopy (AFM), and small-angle X-ray scattering (SAXS), which can provide complimentary information regarding their cross-sections, length, and distributions. In addition, solid-state ^{13}C cross-polarization magic-angle spinning nuclear magnetic resonance (CPMAS NMR) and wide-angle X-ray diffraction (WAXD) can be used to determine the crystalline structure and crystallinity of cellulose nanofibers. An extensive survey of characterization methods for cellulose nanomaterials has also been recently published.[98]

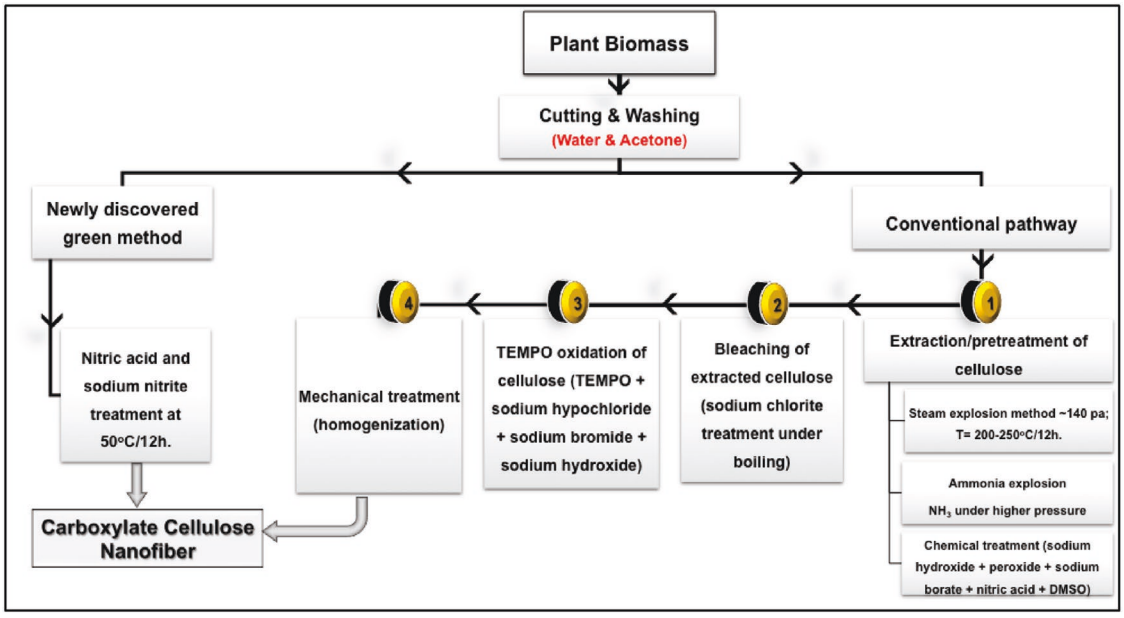

Figure 9. Process diagram comparing the conventional TEMPO-oxidation and nitro-oxidation methods to extract nanocellulose from untreated biomass.

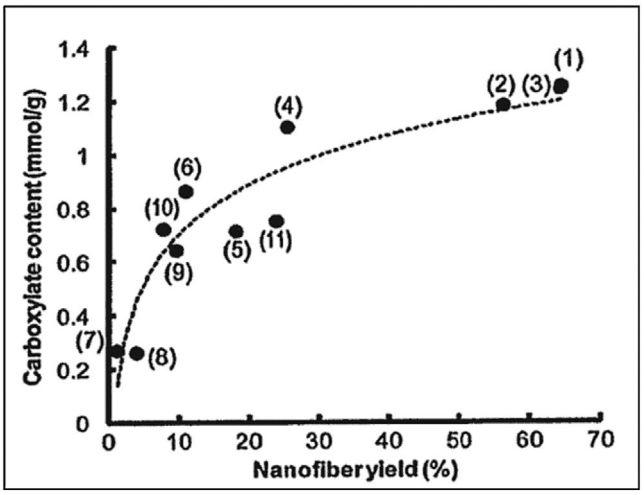

Figure 10. Relationship between the carboxylate content and CNF yield prepared with various TEMPO-derived catalysts. Reproduced with permission.[101] Copyright 2010, Elsevier.

When it comes to TEMPO-oxidized CNF, its cross-sectional dimensions and length distributions can be determined with reasonable accuracy.[66,99] However, less defibrillated and coarser nanocellulosic materials are inherently more difficult to characterize. For nanocellulose membrane applications, more defibrillated materials or nanofibers with higher L/D (aspect ratio) values are more suitable. As a result, fast and simple procedures to separate out CNFs with different L/D distributions are very useful, and some procedures have been demonstrated.[100,101] Typically, these procedures are based on the centrifugation of CNF suspensions under a certain set of conditions, where CNFs should have a sufficient colloidal stability. For charged colloidal systems, these conditions can be achieved at low ionic strengths. In **Figure 10**, the relationship between the apparent yield obtained by centrifugation of various TEMPO-oxidized CNFs is presented.[101] As the carboxylate content increases, the CNF yield also increases, meaning there is more efficient defibrillation of cellulose fibers. Such a diagram can be used to guide nanofiber production with a similar oxidation process to extract CNFs.

4. Nanocellulose-Enabled Membranes for Water Purification

4.1. Role of Nanocellulose in Filtration Membranes

Earlier, we illustrated the relationships between pore size and pressure for pressure-driven membranes (Figure 1). If one considers the CNF dimensions (cross-section size: 2–10 nm and fiber length up to a few micrometers), it is immediately clear that these nanomaterials are suitable for construction of barrier layers in pressure-driven membranes (MF and UF) with defined mean pore sizes. The dimensions of CNFs are in a similar range as those of carbon nanotubes (CNTs) and electrospun nanofibers (CNFs have a much longer fiber length than CNTs, and CNFs have a much smaller cross-sectional size than electrospun nanofibers), where the latter two have already been demonstrated as effective nanomaterials for barrier layer fabrication in the design of new filtration membranes[102] Several excellent reviews and book chapters have been published that deal with this subject.[102,103,104]

A schematic diagram is provided in **Figure 11** to show the type of membrane, selectivity for contaminant removal, and possible configuration of nanofiber membranes involving CNFs. These designs are based on our experience using electrospun nanofibers,[17] made of synthetic polymers such as polysulfone, polyacrylonitrile, polyvinylidene fluoride, and poly(acrylonitrile)–poly(vinyl chloride) copolymers, and CNTs for water purification membranes. In the MF membrane design, we believe the infusion of CNFs into a cellulose microfibrous scaffold is an effective way to fine-tune the pore size without drastically decreasing the porosity.[17,19,105] In a way, the void in the microfibrous scaffold is partially filled with CNFs, where the mean pore size and the pressure drop can be adjusted by the loading of CNF content. The barrier layer is formed by the resulting composite structure of nanofibers and microfibers, where functional CNFs can further offer adsorption functionality. Several recent articles have been published that demonstrated MF membranes with simultaneous filtration and adsorption capability.[4,44] We believe this configuration will be particularly useful for gravity-driven filtration operations in off-grid environments.

In UF membranes, the barrier layer should be fabricated directly from CNFs. This is illustrated in Figure 11, where a

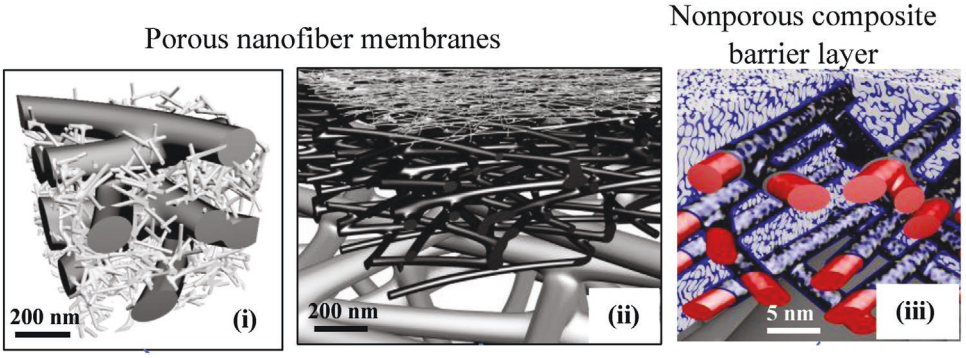

Figure 11. Possible designs for pressure-driven membranes: i) MF (microfiltration); ii) UF (ultrafiltration) and NF (nanofiltration); and iii) RO (reverse osmosis) using cellulose fibers with different cross-sectional dimensions.

three-layered thin-film nanofibrous composite (TFNC) structure[16] containing fibers of different diameters is shown. The mean pore size of the barrier layer in the TFNC membrane is directly related to the barrier layer thickness if the CNF dimensions are fixed. In later sections, we will discuss the parameters that can control the pore size and porosity of the barrier layer in these membranes.

In NF/RO membranes, nanocellulose can also play a role; however, it is in a less direct manner. It has been demonstrated that nanocellulose (CNFs and CNCs) can be embedded in the matrix (e.g., cross-linked polyamide formed by interfacial polymerization) of the barrier layer and form an interconnected fibrous scaffold. As a result, interconnected "directed water channels" can be formed between the nanofibers and matrix in the barrier layer.[106,107] These channels are quite different from the existence of "free volume" in the tightly cross-linked structure of conventional polyamide matrix, often resulting in low flux performance. The introduction of directed water channels can lead to an increase in permeance (permeation flux normalized by membrane thickness) without loss of selectivity.

Nanocellulose is not only useful for the design and construction of nanofibrous membranes driven by a pressure gradient (MF, UF, NF, and RO), but it is also suitable for those driven by a concentration gradient (ΔC), as in forward osmosis (FO);[108] by a temperature gradient (ΔT), as in membrane distillation (MD);[109] or even by an electric gradient (ΔE), as in electrolysis.[38,110] In the latter cases (FO, MD, and electrolysis), the separation principal is mostly based on size exclusion, where the performance of the membranes is closely related to the pore size, pore size distribution, porosity, tortuosity, and thickness of the barrier layer, which will be discussed later.

4.2. Other Nanocellulose Technologies Relevant to Membrane Fabrication

Since the first development of microfibrillated cellulose,[70] nanocellulose technologies have offered a myriad of opportunities for new biomass applications. Initially, microfibrillated cellulose was targeted toward food processing (rheology) and paper strength applications. For example, the first known publication on the use of nanocellulose in papermaking was based on bacterial cellulose,[111] where a drastic increase in the Young's modulus (>15 GPa) was observed. This work immediately inspired the use of nanocellulose for making films, membranes, nanopaper, and nanosheets. Unrivaled performance and results further came into sight when more exquisite forms of nanocellulose (Table 2) were developed and utilized. Undoubtedly, the development of TEMPO-oxidation technology has paved the way for more high-tech applications of nanocellulose (CNFs).[66,112]

The most common approach to using nanocellulose is in nanocomposites,[113,114] as it has long been realized that even small additions of nanocellulose can enhance the properties of composite materials quite significantly.[115] Nanocellulose films/membranes, such as MFCs, CNFs, and CNCs (or NCC) often exhibit outstanding properties, including high mechanical strength,[116] low thermal expansion coefficient,[117] high optical transparency,[118] good gas barrier properties,[119] good chemical resistance, low environmental impact, and functionality,[49,120] which make them attractive materials for packaging application.[121] Nanocellulose films are also referred to as nanopaper, which Henriksson et al. (2008) defined as a network composed of intertwined nanofibrils in the fashion of random-in plane orientation.[122] Technically, the film term is appropriate only for a very thin, dense, less porous substrate, while the membrane term is appropriate for a porous thin substrate with high permeability. Generally, nanopaper is produced using papermaking techniques that involve passing the nanocellulose suspension through a microfiltration apparatus under vacuum, occasionally followed by hot pressing.[34,44,123–125] As a result, nanopaper is mechanically robust and possesses low porosity and small pore size. Nanopaper has also been targeted for design in such a way that it can act as a membrane or an adsorbent.[47]

The usefulness of nanotechnology for water remediation has been known for over a decade.[104,126] However, only in the past few years have researchers realized the potential of using nanocellulose for varying water purification applications,[4,48,127] including membrane filtration.[8,9,123,125,128–132] Recently, a few developments have been made to design nanocellulose membranes to adsorb heavy metal ion impurities.[40,133] However, to realize the full potential of nanocellulose for fabrication of water filtration membranes, it is necessary to have a sound understanding of the process, structure, and property relationship for nanocellulose membranes based on our knowledge of the cellulose technologies in papermaking. In the following section, the most relevant membrane properties for water filtration are discussed.

5. Tailoring the Relevant Nanocellulose Membrane Properties for Water Purification

To tailor the performance of nanocellulose membranes for water filtration, we consider four major properties here 1) dry membrane strength, 2) wet membrane strength, 3) membrane pore size, and 4) membrane porosity. The principle and some common approaches that can be used to control these properties are discussed as follows. In (1) and (2), the mechanical performance requirements for handling (dry strength) and operating under high pressure in an aqueous environment (wet-strength) of conventional membranes have been well documented[5–11] and will not be discussed here. However, these performance matrices will serve as benchmarks for us to develop suitable nanocellulose-enabled membranes for various water purification applications.

5.1. Dry Membrane Strength

The dry membrane strength is an important property, as the membrane integrity must be maintained during handling. It is well known that fibers are invariably stronger than the same material in bulk (e.g., solid films), which is particularly true for brittle materials such as nanocellulose. Typically, packing of fibers into a bulk material cannot prevent the presence of voids, and there may be additional surface defects and internal stresses imposed during manufacturing. Unfortunately, for

nanocellulose, as a fairly new type of material, none of these considerations have been taken into account. There have been no estimations of the maximum strength or stiffness of nanocellulose films, even though there has been extensive modeling activity with respect to nanocellulose starting in the early 1990s.[115,134]

The mechanical properties of cellulose nanopaper was recently reviewed by Benitez and Walther[114] and Ansari et al.[135] These reviews focused on the current state-of-the-art technologies and understanding related to the mechanical performance. Lindstrom has suggested a simple fashion by which the tensile properties of CNF nanopapers can be described by the Page equation developed for paper materials.[87] The effects of various parameters (which are often interconnected), including the degree of polymerization (DP),[122,136] width of nanofibrils,[15,34] length of nanofibrils,[99] film thickness,[130,131,137] and post-treatment conditions[123] on the mechanical properties of nanopapers have been discussed; these can provide clear guidelines for fabrication of robust nanocellulose filtration membranes. In addition, the thermal and wet stability can also affect the filtration performance. A recent study clearly showed that mechanically weak membranes can rupture at high pressures and temperatures during filtration, which would negatively affect the performance.[8]

In the context of the classical papermaking process, there was a golden standard for understanding the strength of paper materials, i.e., the Page formalism.[138] The Page equation involves some primary factors responsible for paper strength: 1) the fiber tensile strength, 2) the specific bond strength (SBS) between fibers, and 3) the relative bonded area (RBA). Several factors, including sheet formation, fiber kinks, material distribution in the *z*-direction of sheets, residual stresses at different structural levels, and the strain during shrinking, are ignored, whereas these factors are known to be important for paper materials, which presumably also holds true for nanopaper materials. The Page equation takes the following form in the ISO nomenclature, which is expressed in Equation (2)

$$\frac{1}{\sigma_T^w} = \frac{9}{8 \cdot \sigma_{\text{Zero}}^w} + \frac{12 \cdot A \cdot \rho}{SBS \cdot P \cdot L \cdot RBA} \tag{2}$$

where σ_T^w is the tensile index (N m kg^{-1}), σ_{Zero}^w is the zero span breaking length (N m kg^{-1}), A is the average fiber cross-section (m^2), ρ is the density of the fibers (kg m^{-3}), SBS is the specific bonding strength or the shear bond strength per unit bonded area (Pa), P is the perimeter of the fiber cross-section (m), L is the fiber length (m), and RBA is the relative bonded area in the sheet (%).

In principle, most of these parameters, except for SBS, are easy to measure. As there are highly developed methods to measure the interlaminar shear strength of paper (σ_{Shear}), its relation to SBS can be simply given in Equation (3)

$$\sigma_{\text{Shear}} / \text{RBA} = \text{SBS} \tag{3}$$

This means that the Page equation can be used to calculate the tensile index directly from first principles, which has been recently verified.[139] The relative bonded area can be conveniently determined by gas adsorption at low temperatures, i.e., by calculating the monolayer surface area at low vapor pressures using the molecular size of the gas. The RBA can then be obtained as

$$RBA_{\text{BET}} = (\text{BET}_o - \text{BET}) / \text{BET}_o \tag{4}$$

where RBA_{BET} is the relative bonded area measured with the BET technique. BET_o represents the BET area for a sheet with a tensile index of zero, which is the surface area of a nonconsolidated sheet.

The Page theory can be extended to nanopapers or nanocellulose membranes by performing a series of experiments using different dry-strength agents on a given nanofiber (e.g., CNFs extracted from bleached softwood Kraft pulp). It has been found that carbohydrate-based dry-strength agents (e.g., starches) only affect the bonded area, and not the specific bond strength. Moreover, the BET area of a nanopaper/membrane is inversely and linearly related to the tensile index. This allows extrapolation of the tensile index to BET area = 0 (i.e., the BET area of a nonporous film). It is interesting to note that the extrapolated tensile strength for a CNF film at zero BET area was 172 Nmg^{-1}, where a sheet of paper made from bleached Kraft pulp also exhibited a short span strength of 174 Nmg^{-1}. Hence, the maximum strength of a nanocellulose film is equal to the short span strength of the fiber material it was made from. In other words, the maximum strength of a nanocellulose film is governed by the nanofiber strength, and not by the bond strength between the fibers. Hence, this simple approach may be useful to estimate the strength of nanocellulose membranes under ideal conditions. For nanocellulose membranes, the maximum strength is dependent on the membrane density, the nature of the nanofiber (e.g., CNC vs CNF), and manufacturing protocols.

We note that there are some limitations regarding the use of the Page equation. For example, the above approach assumes 1) the fibers have been sufficiently defibrillated, but the degree of polymerization in nanocellulose is not excessively decreased, and 2) the fiber angle is low for the used pulp, by which the short span strength is determined. These assumptions seem to hold for most nanocellulose films (from bleached Kraft pulps), as a survey of the literature indicates that their maximum strength ranges from 165 to 185 N m g^{-1}.[87] This strength range may be due to the local grammage variation or the nanofiber distribution in the film plane. The film properties, however, become much more complex when the counterion on the nanofiber is changed. It is known that nanocellulose can be negatively charged in a film in an aqueous environment. In the presence of Na^+ ions (most commonly encountered), colloidal aggregation of nanocellulose can occur, resulting in deterioration of film properties.[140] Different alkali ions (e.g., Li^+ and Cs^+) give different results, where a larger ion diameter can yield a lower tensile strength but a higher strain-to-failure ratio. This has been interpreted by inelastic deformation mechanisms, where larger counterions bound to the fiber surface would induce interfibrillar sliding and reduce the binding strength between the nanofibers.

5.2. Wet Membrane Strength

It is well known that nanocellulose films (or nanopapers) are extremely sensitive to humidity. When they are soaked in water,

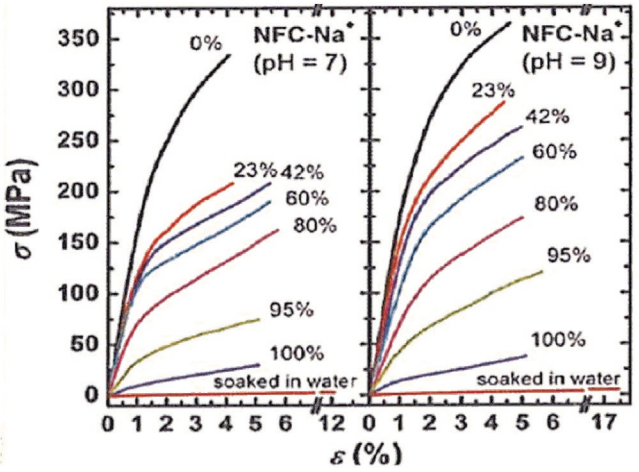

Figure 12. Mechanical properties of nanocellulose films from TEMPO-oxidized nanocellulose as a function of humidity. Reproduced with permission.[142] Copyright 2013, American Chemical Society.

the films lose all their integrity, as illustrated in **Figure 12**. This constitutes a major challenge if nanocellulose membranes are to be used as nanofilters in aqueous applications. There are several different approaches that can be used to alleviate the moisture sensitivity of nanocellulose membranes. We note that wet-strengthening of papers, a major approach for this purpose, is in itself a fairly mature field, where extensive research has been conducted over the years,[141] and the reader can find a large list of references with appropriate reviews. Here, some selected routes for wet-strengthening nanocellulose membranes are discussed.

5.2.1. Wet-Strength Resins

Commercial wet-strength resins in papermaking can be used to improve the integrity of nanocellulose membranes in water. These resins are divided into two groups: temporary and permanent. Permanent resins are generally able to form covalent bonds, which are not readily hydrolyzed in water; temporary resins are usually based on reactive aldehydes that form acetal or hemiacetal linkages with cellulose. For example, in the case of cellulose nanopapers, it has been shown that TEMPO-oxidized nanocellulose films contain aldehyde groups, which can crosslink. However, these crosslinks often fail to give permanent wet-strength improvement.[143]

Commercially available permanent wet-strength resins can also be divided into the following groups: urea-formaldehyde and melamine resins, alkaline curing polymeric amidoamine-epichlorohydrin resins, and glyoxalated polyacrylamide resins. Historically, urea-formaldehyde and melamine resins have dominated the field, but today, the polymeric amidoamine resins have come to dominate the market. The most important resins in this group are derived from secondary amines and have 3-hydroxy-azetidinium rings as their principal reactive group.[144] These resins have been applied to improve the wet-strength of nanopapers based on TEMPO-oxidized nanocellulose.[145] The reactivity of the azetidinium ring with carboxyl groups on cellulose is essential for attaining high wet strength.

In the literature, many experimental wet-strength resins have been reported, including chitosan,[146] aqueous phenol formaldehyde,[147] polyethylene oxide (PEO),[148] and water-soluble polysaccharides.[149] The chemistry involved with the use of these polymeric resins always depends on the interactions (physical or chemical) between the functional groups on the resin and those on the nanocellulose.

5.2.2. Cross-Linking Agents

The primary difference between wet-strength resin and cross-linking agent is that the former is usually a polymer, and the latter is a reactive low molecular agent. In addition, the amount of cross-linking agent used is usually much less than that of wet-strength resin. However, the difference between the two can be vague in some instances.

As extensive work has been done in the textile industry regarding the use of polycarboxylic acids for manufacturing wrinkle-resistant cotton fabrics, this approach has also been applied as a wet-strength agent for papermaking.[141,150] To impart ester formation, high temperatures and a suitable catalyst (e.g., sodium hypophosphite) are needed for curing, where the procedure has been shown to give good wet-strengthening improvement, but it also results in brittleness of the cured materials. In the case of membranes prepared from TEMPO-oxidized CNFs, the aldehyde groups that form during the TEMPO-mediated oxidation process can also act as cross-linkers while drying at an elevated temperature (e.g., ≈110 °C for 15–20 min).[151,152] The high aldehyde content and proper cross-linking conditions can improve the wet strength of the membrane. Many cross-linking agents have been reported for nanocellulose, including citric acid, low-molar-mass polyethylenimine (PEI),[131] inorganic salts[153] (calcium chloride, sodium trimetaphoshate), glutaraldehyde,[46] $CaCl_2$ treatment,[154] and glycidyl trimethyl ammonium chloride.[155] The chemical interactions between nanocellulose and cross-linking agents are usually covalent or ionic in nature. Finally, light-induced cross-linking reactions is also an effective route to improve the wet strength of nanocellulose membranes.[156] In particular, the presence of benzophenone can initiate radical-based cross-linking reactions in the nanocellulose scaffold under UV radiation. This approach offers several advantages, such as higher stability compared with other photo cross-linking agents, including diazo esters, aryl azides, and diaazirines, and can be activated at 350–360 nm to react preferentially with unreactive C—H bonds in cellulose.[157]

The use of a cross-linking agent can greatly improve the wet strength of the membrane, but it may also affect other membrane properties (such as pore size and environmental stability). For example, membranes prepared from *Cladophora* nanofibers are usually suitable for microfiltration. However, when the membrane was cross-linked with citric acid, followed by hot pressing, the corresponding pore size decreased to less than 20 nm, making it suitable for ultrafiltration or even nanofiltration.[9] In another study, the use of a pH-sensitive cross-linking agent (e.g., PEI) was found to result in low pH intolerance for membranes based on NMMO–cellulose nanofibers.[131,158]

5.2.3. Counterion Approach

The counterion interactions in charged nanocellulose suspensions have a significant impact on the rheology of the gels. In general, the pH level, counterion valence, and concentration,[159] as well as counterion size,[140] all can affect the colloidal interactions between charged nanocellulose particles. Thus, there are two different pathways to control the wet strength of the membranes. One is adding counterions directly into nanocellulose suspensions and using the gelation property to control the structure and property during membrane formation. The other pathway is adding counterions into nanocellulose membranes, allowing ionic cross-linking reactions to take place as a post-treatment procedure. For example, the ion exchange of monovalent sodium ions in a formed nanocellulose membrane with multivalent ions should significantly enhance its water resistance. Both pathways can radically change the permeability of the membrane;[160] thus, fine-tuning the ionic interactions and the pore-size distribution must be carefully achieved to optimize the wet strength and filtration performance.

5.2.4. Hot Pressing

Hot pressing of CNF nanopaper under certain temperatures for a longer time can increase the wet strength and the barrier properties of the resulting film.[161] This is because the drying of nanopaper under hot pressing will effectively induce irreversible hornification, a well-known phenomenon that leads to cocrystallization of cellulose chains.[162] In one study, an increase in drying time during hot pressing from 0.5 to 2 h increased the tensile strength from ≈120 to ≈225 MPa at a similar strain-to-failure rate of ≈6%. Additionally, the hot-pressing process has often been used to prepare chemically resistant CNF films.[163] However, the increase in heat exposure while the membrane is in the wet state can cause a decrease in the porosity of CNF membranes, along with an increase in the Young's modulus.[164]

5.2.5. Cramping/Wrinkling of Membranes

The cramping/wrinkling of membranes during drying can be an issue during fabrication of nanocellulose membranes.[165] It is well known that, in papermaking, the transversal shrinkage, induced by the interfibrillar swelling of cellulose chains, can induce film shrinkage of up to 20%. This behavior will induce wrinkling, particularly when the *z*-distribution of cellulose materials and the density gradient are profound. This issue, however, can be avoided when the paper is held under restraint. Nanocellulose fibrils are not subjected to transversal shrinkage if the fibers have been fully delaminated. Less delaminated fibers, will, however, induce transversal shrinkage, which can be important for wrinkling of nanocellulose membranes.[159] Less defibrillated fibers, however, will induce transversal shrinkage and can became problematic for wrinkling of nanocellulose membranes. Semicommercial roll-to-roll fabrication of nanocellulose membranes can avoid wrinkling of the membrane.

Although there are very few descriptions in the literature resolving the cramping issue, one practical solution is that the problem can be avoided by the use of ring holders. The holder can restrain the membrane/film shrinkage during drying without affecting the surface morphology of the membrane. In addition, aggregation of fibers during forming can also result in heterogeneous structures in the membrane with deteriorated properties caused by the nonuniformity. Until now, there have been very few studies describing solutions for this issue. We believe the use of optimized cellulose nanofiber concentrations can help to solve this problem.

5.2.6. *z*-Directional Material Distributions

If a papermaking type of manufacturing is considered for membrane fabrication, the material distribution in the *z*-direction will be governed by water retention (and the use of retention/dewatering adjuvants) and dewatering.[166] As the dewatering content increases, the top and bottom surfaces of the membrane can be devoid of the smallest nanocellulose fragments as a result of mechanical entrapment mechanisms. If retention aids are used, the nanomaterial distribution may be more even in the *z*-direction of the membrane, but the membrane formation will grow worse.

5.2.7. Long Filtration Time for Nanocellulose Filtration Membrane

The long usage of nanocellulose membranes during filtration will be the biggest challenge hindering practical applications of these membranes during industrial operation. The long filtration times for nanocellulose filtration membranes, however, can be improved by overpressure techniques, where the pressure is exerted at the top of the sample unit to make the filtration faster.[163] In addition, the coagulation/flocculation process of CNFs with polymers/multivalent ions before filtration can help improve the rate of dewatering.[34] For paper materials, mathematical modeling has shown that the pore size distribution in paper is sensitive to the paper formation process, and it is expected that this also holds true for nanocellulose materials.[167]

5.3. Membrane Pore Size

The membrane pore size is an essential parameter related to the membrane performance. Typically, as the pore size decreases, the selectivity or rejection ratio increases. In the previous sections (Sections 5.1 and 5.2), we discussed different methods to enhance the membrane strength. These methods would inevitably reduce the membrane pore size. In this section, we outline some effective approaches that can control the porosity of nanocellulose membranes.

5.3.1. Effect of Nanofiber Cross-Sectional Dimensions or "Diameter"

The cross-sectional dimensions (or effective "diameter") of nanocellulose (e.g., CNFs) can significantly affect the pore size

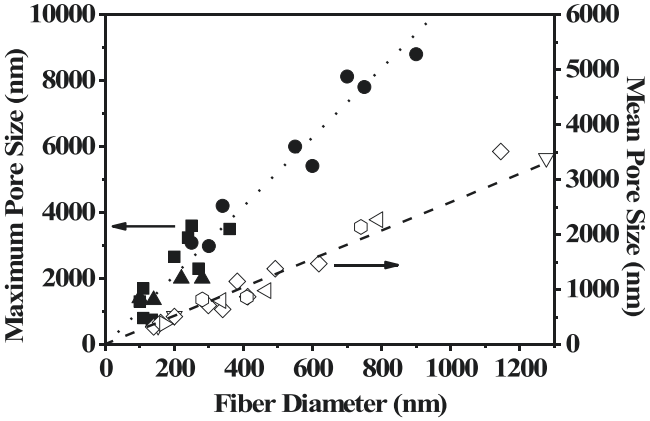

Figure 13. Correlation between the maximum pore size, mean pore size, and mean fiber diameter in optimized nanofibril scaffolds. Reproduced with permission.[15] Copyright 2012, American Chemical Society.

of the resulting membrane. It has been well recognized that nanocellulose typically does not have a cylindrical shape, but rather shows a square[66] or ribbon/rectangular[168] shape. However, if one considers that nanocellulose has a nominal "diameter," it has been found that CNFs with diameters in the range of 3–6 nm can produce a thin membrane barrier layer with a mean pore size on the order of 20 nm.[15,17] These membranes are suitable for MF and UF applications. Ma et al.[15] reported that there is a linear relationship between the mean pore size (as well as the maximum pore size) and fiber diameter for an optimized barrier layer (i.e., with the thinnest possible but uniform thickness) based on electrospun PAN and PES nanofibers (**Figure 13**). The mean pore size increased with an increase in fiber diameter (the mean pore size is approximately three times that of the nanofiber diameter in electrospun scaffolds). Zhang et al. also confirmed that the pore size of a packed interfibrillar network is closely related to the diameter of a cylindrical fiber using computational modeling.[169] The relationship in Figure 13 may not be applicable for nanocellulose membranes, as the hydration effect or the solvent flexibilization effect can bend fibers and consolidate the membrane through capillary action. Nevertheless, the close relationship between the pore size and the fiber diameter can still be useful to guide the assembly of CNFs in the nonwoven format. For example, membranes with a thickness of ≈30 nm, constructed by nanofibers extracted from *Cladophora* cellulose, exhibited a mean pore size of ≈30 nm.[10] The *Cladophora* nanofibers were quite thick and stiff, where the capillary action during drying could not result in a large extent of membrane consolidation, resulting in a relatively high specific area. The fiber diameter also seems to affect the membrane strength. For example, Zhu et al. investigated nanopapers with different nanofiber diameters and found that the strength and toughness of these films simultaneously increased with a decrease in fiber diameter (ranging from 27 μm to 11 nm).[170]

5.3.2. Effect of Nanofiber Length or Degree of Polymerization

The nanofiber length is indirectly related to the degree of polymerization (DP) of cellulose chains. A longer fiber generally has a higher number of repeating units in the chains and a higher DP value. The nanofiber length (thus DP) can also affect the pore size of the resulting nanofiber membrane. Longer fibers generally possess more kinks, which can lead to larger interfibrillar gaps during drying. This would lead to a larger membrane pore size. In contrast, shorter fibers typically manifest themselves into a more compact form during drying, resulting in a smaller pore size. However, we anticipate that the effect of the fiber length on the pore size is much smaller than that of the fiber cross-sectional dimension. The DP of the nanofibers can also affect the membrane porosity.[122] For example, cellulose fibrils with a DP of 410 exhibited a membrane porosity of 20%, while fibrils with a DP of 1100 showed a porosity of 28%.[122]

5.3.3. Templating Method

One can control the pore size, the uniformity of the pore, and the wet strength of nanocellulose membranes by the templating method. For example, calcium carbonate particles with desired sizes have been used as templating agent during the membrane fabrication of nanocellulose. The embedded particles were subsequently removed by acidic washing, leaving behind desired sizes of pores in the membrane.[125] In another study, $AlCl_3$ was employed as a coagulating agent to facilitate the preparation of nanopapers using TEMPO-CNFs, bacterial CNFs, and CNCs using the vacuum filtration technique, where all the resultant nanopapers exhibited a pore size of 19 nm, suitable for ultrafiltration.[34] The use of $AlCl_3$ greatly increased the permeability of the nanopapers, which is essential for UF membranes.

5.3.4. Effect of the Drying Rate

As cellulose is thermoplastic under moist conditions,[67] the most important processing parameter that can affect the membrane pore size is the rate of drying. Other parameters, such as the drying temperature, membrane thickness, water content, and applied force, can also play a role on the pore size.

Recently, Gustafsson et al. investigated ways to fine-tune the pore size of membranes prepared from *Cladophora* nanofibers through altering the temperature and film thickness using the hot-press drying approach,[123] where the pore size could be tailored between 10 and 25 nm. Their study indicated that a slower drying rate could result in a smaller pore size in the membrane. This observation can be understood by the concept of capillary action (because of the flow of free water), which provides the primary attraction force between the nanofibers. When the nanofibers come close together and develop more contact areas, the secondary attraction forces, such as hydrogen bonding and van der Waals attraction forces, can also come into play. The capillary forces, also termed Campbell forces[171] in the papermaking community, are extremely strong. They have been shown to be very effective, even down to the length scale of 4 nm under clean conditions.[172] At a faster drying rate, air percolation can occur, and this effect would block capillary action and increase the residual pore-size distribution. However, at a faster drying rate, the effect of surface plasticization (resulting

from bound water) can also take place on nanocellulose, counteracting the effect of air percolation. The latter is usually dominant at the final stage of drying, leading to a denser membrane with low porosity. In contrast, at a slower drying rate, even though the capillary action would continue (also at a slower rate), the fiber entanglement is still a dominant factor, resulting in a relatively loose fibrous structure or a higher porosity.

It was found that in thicker membranes, there is less chance for air percolation to take place. Thus, sufficiently thick nanocellulose membranes are basically nonporous in the dry state.[173,174] In contrast, during drying of sufficiently thin nanocellulose membranes, air percolation often takes place, which will block further capillary action and increase the residual pore-size distribution after drying. This will, however, not be the case if the nanocellulose film is coated on a nonporous surface, such as a Petri dish.[173] In this case, the gas permeability is independent of film thickness.

5.3.5. Surface Coating Method

The pore size of a nanofiber membrane can be controlled by the surface coating method. In short, a thin barrier layer having the desired pore size can be cast on the nanofibrous scaffold, which is a highly effective way to reduce but control the overall pore size of the membrane. As the thickness of the barrier layer is inversely proportional to the permeation flux,[125,130,131] the smallest thickness for the barrier layer is preferred. There are many coating techniques that are suitable for this purpose, including knife casting, slot die coating, and solution spraying techniques, just to name a few.[175] To achieve a uniform coating with the smallest layer thickness, a dilute and homogenous solution/suspension of the coating material is required. It is essential not only to control the concentration of the coating material, but also to make sure that the coating layer does not penetrate into the supporting scaffold, which could greatly reduce the permeation flux. The proper selection of the coating material can significantly enhance the rejection ratio or selectivity, but the thin coating layer thickness will not sacrifice the flux performance.[5] In addition, the coating of a hydrophilic barrier layer can often increase the fouling resistance by reducing the particulate clogging and adsorption of hydrophobic foulants, leading to membrane longevity.[176]

5.3.6. Determination of the Membrane Pore Size

There are several methods that can be used to effectively determine the pore size of a membrane. In the dry state, the average pore size can be characterized by positron annihilation lifetime spectroscopy (PALS). It has been shown that the average pore size of TEMPO-oxidized nanocellulose membranes is ≈0.47 nm,[173] making them useful for gas separation.[42] However, in the wet state (as in water purification), the pore size of the membrane is generally determined by two methods, the porometry (e.g., capillary flow porometry)[177] and molecular weight cutoff (MWCO)[178] methods, depending on the range of the pore size. The principle of the porometry technique is based on the displacement of a wetting liquid from the pores of the membrane by applying an inert gas at increasing pressure. With this technique, the minimum, maximum, and mean flow pore sizes, as well as pore size distribution, of the membranes can be determined, where the measurable pore size range is from 500 μm to 10 nm (i.e., up to UF range).[177] The MWCO method is a characterization technique typically used to determine the pore size and distribution at a much smaller scale (1–10 nm, i.e., UF to low-end NF range). As macromolecules can be characterized by their molecular weight, MWCO is defined as the lowest molecular weight of the chosen solute macromolecules, in which 90% of the solute is retained by the membrane. Typical solute macromolecules include dextran and polyethylene oxide (PEO).

5.4. Membrane Porosity

There are several methods that can be used to effectively control the porosity of nanocellulose membranes, which is directly related to the permeation flux or permanence. One of those methods is the templating technique, which will not be discussed here. This is because with the templating method, if the content of the imbedded salt particles in the nanocellulose membrane increases, the resulting porosity will also increase. We here discuss two common methods that can control the membrane porosity.

5.4.1. Solvent Exchange Method

The solvent exchange method involves the replacement of water with a less hydrophilic solvent during membrane fabrication. This method can be effectively used to control the membrane porosity (also the pore size). Typically, applicable solvents include methanol, acetone, ethanol, and *tert*-butanol. These solvents can reduce the intra- and interfibrillar interactions, increase the fiber stiffness, and decrease the capillary forces between CNFs.[122,124,125,179] It has been reported that the solvent exchange of water with acetone in the wet state of a membrane can increase the membrane porosity to 40%, as compared with 19% in water. Similarly, the porosity of membranes was increased to 28% and 38% when water in the membrane was exchanged with methanol and ethanol, respectively.[122] However, even though the solvent exchange method can lead to an increase in the membrane porosity, it will cause a decrease in the membrane strength.[124] In addition to solvent exchange in the wet state, drying of the nanocellulose membrane by liquid CO_2 evaporation was also found to increase the porosity to 74% because of the decreased capillary action resulting from the low polarity of CO_2.[124] The freeze drying technique is another way to control the porosity of the membrane.[124]

5.4.2. Effect of Membrane Thickness

In nanocellulose membranes, the membrane thickness is a major factor affecting the porosity of the membrane,[130,131] which is directly related to the permeation flux. As the membrane thickness decreases, the permeation flux increases (they

are inversely correlated). The membrane thickness can be controlled by the amount of nanocellulose suspension used during fabrication (e.g., vacuum filtration). However, a change in the membrane thickness will also affect other properties. For example, it has been observed that nanopapers with the same density but different thicknesses exhibit different transparency and Young's modulus values. Specifically, thinner films often exhibit a higher transparency, and thicker films have a lower Young's modulus.[130,131,137] In addition, thicker films can possess a higher residual stress because of the composition gradient resulting from the drying process, which can decrease the modulus.

6. Current state of Nanocellulose Membrane Development for Water Filtration

Many different methods for making nanocellulose membranes at the laboratory scale have been demonstrated over the years. These methods include room-temperature or oven drying of membranes by evaporation in Petri dishes and the like;[173] vacuum filtration of nanocellulose suspensions and drying;[73,180] applications of papermaking procedures using Rapid-Köthen sheet former equipment[181] or dynamic sheet-formers such as dynamic sheet-former equipment (Formette Dynamiqe, France); or hot-pressing procedures.[182] Forming, pressing (dewatering), and drying are challenging manufacturing operations, whereby at the moment, there are no upscalable inexpensive, simple, and fast procedures for the integrated manufacture of nanocellulose membranes. A more simple approach to apply nanocellulose is to use it as a coating material.[174,183] This turns out to be a useful procedure for making thin layers of nanocellulose coatings as the barrier layer for filtration membranes.[151,184]

In spite of the above challenges, nanocellulose membranes have been shown to be effective media for pressure-driven filtration operations, such as MF,[17,43,187] UF,[9,16,46,107,34,151,185] and NF.[43,131,152] The usage and challenges associated with nanocellulose membranes are presented in the following section. Membranes fabricated using nanocellulose can be designed for various filtrations (MF, UF, and NF) by alteration of the mean pore size of the membrane. Studies have shown that the membrane pore size can be regulated by the fiber dimensions,[16,99,34] degree of polymerization in the fibers,[122] membrane thickness,[130,131] membrane processing,[44] cross-linking and fillers,[46,131,153,154] which have been discussed above. Specific examples of nanocellulose membranes for MF, UF, and NF applications in different formats are described in this section. For RO (and high-performance NF) operations, nanocellulose coating layers have been found to be a unique scaffold to support the fabrication of an interfacially polymerized polyamide (PA) barrier layer. The resulting nanocomposite nanocellulose/PA barrier layer can introduce directed water channels to improve the permeance of the membrane,[106] which will also be discussed later.

We envision that nanocellulose membranes can also be used in concentration-driven FO operation, where the high flux advantage in nanocellulose membranes may further decrease the energy consumption; as well as in thermal-driven MD operation, where the lower cost of nanocellulose membranes may facilitate the dissemination of technology for drinking water purification in remote areas using solar power. We note that for MD operation, one side of the nanocellulose membrane must be modified to become hydrophobic. Unfortunately, none of these membranes have been demonstrated for water purification at the moment.

In the following sections, the current state of nanocellulose membrane development is reviewed based on the format of nanocellulose-enabled membranes: self-standing membranes, or as a barrier layer in composite membranes.

6.1. Self-Standing Membranes

Solvent casting or vacuum filtration are common methods to produce self-standing nanocellulose membranes. The solvent casting method is a simple and fast process, where a nanocellulose suspension or cellulose solution (if the regeneration/precipitation process is used) is cast on a flat surface, after which the solvent is allowed to vaporize at room temperature or at high temperatures. Conversely, the vacuum filtration method is a slow process, requiring the nanocellulose suspension to be filtered through a microfiltration membrane (e.g., 0.2 or 0.4 μm, PVDF or PTFE microfilter) under vacuum. Both processes generally lead to small membrane pore size (mean value > 20 nm), depending on the source of nanocellulose used.

In **Table 3**, we summarize a list of self-standing nanocellulose membranes demonstrated in the recent literature for water purification. The table includes the membrane composition, membrane thickness, membrane porosity, filtration conditions, final permeation flux, and rejection ratio. For example, algal cellulose (*Cladophora*) and bacterial cellulose fibers are natively of high aspect ratio with an average fiber diameter >30 nm; hence, these fibers have been directly utilized to fabricate UF membranes that can also remove viruses and some metal ions.[8,123,34] *Cladophora* nanofiber membranes with slightly different pore sizes (e.g., 19 and 14–24 nm) were prepared by altering the temperature during hot-press drying, whereby the membrane with a mean pore size between 14 and 24 nm and thickness of 21 μm showed 99.9% rejection of viruses with a pure water permeation of 34 L m^{-2} h^{-1} bar^{-1}.[123] The crosslinking of *Cladophora* nanofibers using citric acid could lead to a decrease in the mean pore size to 2–30 nm, resulting in improvement of the separation capability (e.g., capable of removing 20 nm size gold nanoparticles).[9] In a different system, nanocellulose produced by the LiCl/DMAc solvent method was mixed with graphene and electrospun into a nanofiber membrane having a mean porosity of 83%. These membranes were tested for filtration of nonpolar solvents, such as toluene, hexane, and petroleum, using the gravity filtration method. The results showed that these membranes exhibited a rejection ratio >99% for all tested solvents.[129]

Nanocellulose membranes prepared using nanocellulose nanofibers supported on an alumina substrate showed an average pore size of 25 ± 12 nm. These membranes can remove ferritin or gold nanoparticles (diameter ≈ 10 nm) from water, with rejection ratios of 93.8% and 82%, respectively.[130] The average pore size of the nanocellulose membrane was greatly

Table 3. Self-standing membranes prepared from nanocellulose.

Membrane	Thickness/grammage	Porosity [%]/pore size [nm]	Test conditions: Feed solution Pressure/temperature/time	Permeation flux Rejection [%]	
TEMPO CNF and cellulose acetate membrane grafted with lysine	–	13.8 nm	Pure water BASE protein 0.1 MPa	123.4 L m^{-2} h^{-1} 93.6%	[128]
Cellulose dissolved in LiCl/DAM, mixed with graphene oxide and electro spun		83%	Pure water Hexane Toluene Petroleum ether	0.96 m^3 h^{-1} m^{-2} 99.4% 99% 99.8%	[129]
Nanocellulose fibers prepared in NMMO; supported on alumina (200 nm thick)	23 nm	2.5 ± 12 nm	Pure water Ferritin Au particles 10 nm 0.5–4 bar/24 h	22.7×10^3 L m^{-2} h^{-1} bar^{-1} 93.8 ± 0.4% 82.6 ± 0.5%	[130]
Nanocellulose fibers prepared in NMMO; supported on 200 nm pore filter; performed interfacial polymerization using PEI and TMC	77.4 nm	0.45 nm	Pure water Aqueous salt (500 ppm) solution $MgCl_2$ $MgSO_4$ NaCl Na_2SO_4 4 bar/30 °C	32.7 L m^{-2} h^{-1} bar^{-1} 89.7% 65.3% 43.6% 39.1%	[131]
Citric acid cross-linked cellulose nanofibers from *Cladophora*	70 µm	2–30 nm	Gold particles (20 nm) suspension in water 37 kPa	–	[9]
Cladophora nanofibers	70 µm	35% 19 nm	Water SIV virus 10–15 kPa	50 ± 2 µL h^{-1} cm^{-2} LRV ≥ 6.3	[8]
Cladophora nanofibers	21 µm	14–24 nm	Pure water Parvovirus 6 bar	34 L m^{-2} h^{-1} bar^{-1} LRV > 4	[123]
Bacterial nanofibers	20 gsm	2.4 nm	Pure water 0.2–0.5 MPa	<20 L m^{-2} h^{-1} MPa^{-1}	[134]
CNC	20 gsm	2.4 nm	Pure water 0.2–0.5 MPa	≈4 L m^{-2} h^{-1} MPa^{-1}	[134]
TEMPO-CNF	20 gsm	19 nm	Pure water 0.2–0.5 MPa	≈4 L m^{-2} h^{-1} MPa^{-1}	[134]
Homogenized-CNF solvent exchanged with ethanol	30 gsm	10 nm	Pure water PEG (poly(ethylene) glycol-5000 kDa 0.5–3.5 bar 100–150 min	51 L m^{-2} h^{-1} MPa^{-1} 83%	[125]
Incorporation of calcium particles in homogenized-CNF solvent exchanged with ethanol	30 gsm	10 nm	Pure water PEG (poly(ethylene) glycol-5000 kDa 0.5–3.5 bar 100–150 min	78 L m^{-2} h^{-1} MPa^{-1} 70%	

Table 3. Continued.

Membrane	Thickness/grammage	Porosity [%]/pore size [nm]	Test conditions: Feed solution Pressure/temperature/time	Permeation flux Rejection [%]	
Cationic CNF in water	50 gsm	37%	Pure water	58.5 L m^{-2} h^{-1} MPa^{-1}	[44]
Cationic CNF solvent exchanged by ethanol	50 gsm	46%	Humic acid-55 mg L^{-1} 0.5–2 bar	476 L m^{-2} h^{-1} MPa^{-1}	
Cationic CNF freeze dried	50 gsm	79%			
Cationic CNF supercritical CO_2 drying	50 gsm	73%			
CNC incorporated with chitosan, cross-linked with glutaraldehyde		13–10 nm	Pure water Dyes	64 L m^{-2} h^{-1} 70–80%	[46]
CNC electrospun with PVDF-HFP	150–200 µm	0.2–0.45 µm	Pure water	10.2 L m^{-2} h^{-1}	[186]
			NaCl	99.9%	
			27 psi		

decreased to 0.45 nm when the membrane was treated with interfacial polymerization between PEI and trimesoyl chloride (TMC) monomer. This membrane showed a good pure water flux of 32.68 L m^{-2} h^{-1} bar^{-1} and salt rejection ratios of 89.7%, 65.3%, 43.6%, and 39.1% for $MgCl_2$, $MgSO_4$, NaCl, and Na_2SO_4, respectively.[131] A composite membrane based on TEMPO-CNF and a cellulose acetate scaffold modified by lysine grafting was also demonstrated, where the membrane exhibited an average pore size of 13.8 nm and a rejection ratio of 93.6% against BSA protein.[128] The TEMPO-CNF membranes could be solvent exchanged using supercritical CO_2 to increase the average membrane pore size (from 5.5–12.4 to 21–36 nm).[124]

In another study, CNFs were transformed to possess cationic functionality for removal of humic acid by filtration. The cationic CNF membrane was prepared by a range of methods, including solvent exchange, supercritical CO_2 drying, and freeze-drying, where the freeze-dried membrane showed the best performance: a maximum rejection ratio of 79% of and a pure water permeation of 51 L m^{-2} h^{-1} MPa^{-1}.[44] In yet another study, a membrane system containing CNCs (or NCC) and chitosan was cross-linked with glutaraldehyde, yielding an average pore size of 10–13 nm. These membranes were tested in dye removal experiments. The results indicate that the membrane exhibited a pure water flux of 64 L m^{-2} h^{-1} and a dye removal efficiency of 70–80%.[46] Additionally, free-standing hybrid membranes composed of TEMPO-oxidized CNFs and graphene oxide have shown promising adsorption capacity for Cu(II) removal with good recyclability and good hydrolytic properties.[187] Recently, a bilayered aerogel scaffold composed of CNFs and CNTs has been demonstrated for sustainable solar steam generation. In this aerogel, CNFs were used as a porous scaffolding material (99.4% porosity) and thermal insulator,[188] and the CNT substrate was chosen for efficient solar utilization (97.5%). The demonstrated aerogel exhibited solar energy conversion of ≈76.3% and solar irradiation of 1.11 kg m^{-2} h^{-1} at 1 kW m^{-2}.[189] Similarly, Chen et al. (2017) developed a wood/CNT membrane system for solar steam generation, where the composite membrane exhibited a high efficiency of 81% solar energy conversion at 10 kW cm^{-2}.[190]

6.2. Nanocellulose in the Barrier Layer of Composite Membranes

Our group at Stony Brook University has developed a new class of thin film nanofibrous composite (TFNC) membranes, containing multi-layered fibrous scaffolds where the top barrier layer is made of nanocellulose or its nanocomposite.[15,17,106,107,185,191] In a study, we demonstrated that the barrier layer based on TEMPO-oxidized CNFs could replace the flux-limited barrier layer (bulk porosity ≈ 50% and surface porosity ≈ 25%) in typical UF membranes fabricated by the phase inversion method. The nanocellulose barrier layer exhibited high porosity (bulk and surface porosity ≈ 70%) with interconnected voids.[15] Based on the fibrous structure, TFNC membranes, containing a barrier layer made of CNFs (diameter ≈ 5 nm), an electrospun polyacrylonitrile (PAN) nanofibrous scaffold (diameter ≈ 150 nm), and a nonwoven polyethylene terephthalate (PET) substrate (diameter ≈ 20 µm) showed a significantly higher permeation flux (i.e., 2–10 times) than a commercial UF membrane (PAN 10 and PAN 400, Sepro) for separation of oil/water emulsions using commercial UF membranes with a similar rejection capability. Higher permeation flux, which is mostly due to the increased surface porosity, means less time is required to filter the same amount of water, which in turn decreases the energy consumption.[15,16] A schematic picture of the TFNC with SEM/TEM images of each fibrous layer is shown in Figure 4. Additionally, the CNF barrier was found to be efficient for removing UO_2^{2+} ions by adsorption.[21]

In the recent literature, the TFNC membrane format was found to be very effective for enhancing the flux performance in MF and UF applications,[16,17,20,107,185,192] and the presence of CNFs (CNCs) could further provide adsorption capability. Some

examples are as follows. A TFNC membrane containing a barrier layer made of TEMPO-oxidized cellulose nanowhiskers and an electrospun PAN/nonwoven PET substrate showed a high adsorption efficiency against crystal violet dye molecules (positively charged) and a good filtration rejection ratio against bacteria (*E. coli* and *B. diminuta* with LRV = 6) and viruses (MS2 bacteriophage with LRV = 2) at low pressure (19.3 kPa).[17] The infusion of CNFs and MCC into the electrospun PAN scaffold supported by a nonwoven PET substrate was found to reduce the mean pore size of the composite membrane from 2.6 μm to a few hundred nanometers, enabling the removal of *E. coli* from water with a retention ratio of 99.99%.[20] Furthermore, CNFs, chitin nanofibers, and a blend of CNF/chitin nanofibers were found to be suitable barrier layers in nanofiber membranes containing the electrospun PAN/nonwoven PET substrate. These three nanofiber barrier layers effectively reduced the pore size of the final membrane to 25, 27, and 14 nm, respectively, which are all suitable for UF filtration to remove oil emulsions from water. The best-performing system clearly exhibited a high flux performance (490 L m^{-2} h^{-1}) while maintaining a high rejection ration ratio (99.6%). In addition, the membrane with a barrier layer composed of a blend of CNF/chitin nanofibers was found to be robust, as it showed a consistent flux performance for 100 h, several times higher than that of a commercial PAN 10 membrane.[185] In another study, 2,3-dicarboxy cellulose (DCC) nanofibers were used as a barrier layer on a porous PVDF membrane substrate, where the composite membrane could successfully reject 35–45 kDa molecules with an efficiency of 74–80%.[193] The barrier layer was further cross-linked with $CaCl_2$ and $Na_3P_3O_9$, reducing the pore size of the membrane to the 10–55 nm range.[153] Based on the above studies, the following advantages of nanocellulose-enabled membranes for MF and UF applications are apparent.

1) In nanofiber membranes, the coarser fibrous supports made of synthetic polymers, such as electrospun scaffolds or melt-blown nonwoven substrates, can all be replaced by fibrous cellulose substrates with appropriate porosity and pore size/distribution. As the nanocellulose barrier layer defines the final filtration performance, the porosity/pore size requirements of the fibrous cellulose substrates are not as stringent, but the wet strength will be critical.
2) The presence of CNFs (as the barrier layer or as the filler) can also offer additional filtration functions, such as adsorption. Typical CNFs contain negatively charged carboxylate groups, which are effective adsorbents for removal of small positively charged particles, molecules, and metal ions. As a result, filters with dual functionality (i.e., filtration and adsorption) can be designed.

The direct application of CNFs as the barrier layer in filtration membranes will have limitations. This is because the typical cross-sectional dimensions or diameter of CNFs are in the range of 4–6 nm, so the resulting mean pore size of a CNF barrier layer having the minimum thickness to yield the best filtration property (i.e., high flux and low rejection) is ≈20 nm.[107,151] This is only suitable for UF applications. For NF applications, the barrier layer thickness must be increased to enhance the rejection performance (a membrane with smaller effective pore size). However, for high-performance NF and RO applications, this strategy is certainly not worthwhile, as the flux advantage of the nanocellulose barrier layer will be sacrificed to gain better rejection properties. Nevertheless, there is another strategy that has been found to be effective for improving the permeance of the barrier layer without losing the rejection capability.

It is well known that nanocellulose (CNFs and CNCs) can form a nanofibrous network and exhibit gelation behavior in water.[194] As a result, these nanofibers can be incorporated in a polymeric matrix to form a nanocomposite barrier layer. The demonstrated methods to incorporate nanocellulose in the barrier layer include interfacial polymerization[152] and direct mixing with cross-linkable monomers[153,154,195] (e.g., polyethylene glycol diacrylate) in polymerization; other methods, such as UV cross-linking techniques, should also be applicable. The resulting nanocomposite barrier layer thus contains an interconnected nanocellulose scaffold, which can offer the following advantage to enhance the permeance of the membrane in NF and RO applications. 1) As the nanocellulose surface usually takes no or limited part in the reaction to form the barrier layer, the occurrence of an interface between water-impenetrable nanocellulose and the polymer matrix will take place. Because nanocellulose forms an interconnected scaffold in the barrier layer, an interconnected interfacial network between nanocellulose (CNFs or CNCs) and polymer is also present. 2) The nanocellulose/polymer interface can facilitate water passage during filtration, termed directed water channels (a schematic is shown in **Figure 14**), thus enhancing the permeance of the membrane. It is conceivable that the gap distance and the nature of the interface (e.g., hydrophilicity and charge density) can be fine-tuned to adjust the selectivity.

Some example studies of nanocellulose-enabled RO/NF membranes are as follows. Interfacial polymerization of m-phenylenediamine (MPD) and TMC was carried out on top

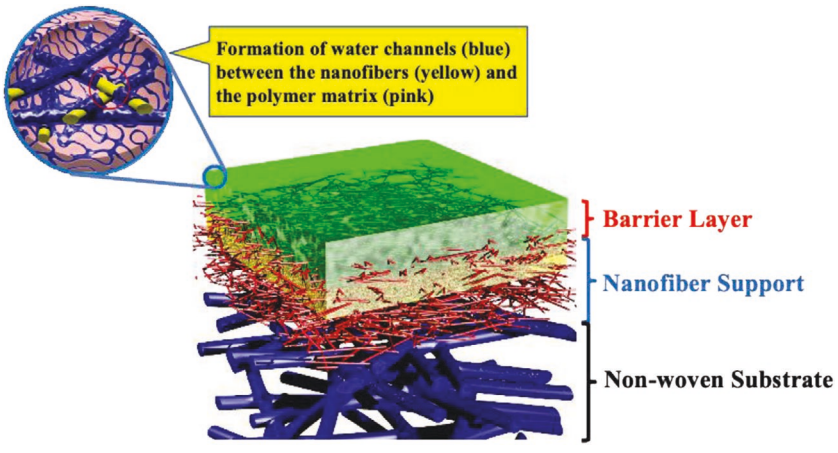

Figure 14. Schematic diagram showing the hierarchical structures of a TFNC RO/NF membrane, where directed water channels (blue) form between cellulose nanofibers (yellow) and polymer matrix (pink) in the barrier layer. Reproduced with permission.[196] Copyright 2014, Elsevier.

of nanofibrous UF membrane substrates (electrospun PAN/nonwoven PET) to create TFNC-style RO membranes. The optimized RO membrane exhibited a rejection ratio of 96.5% against NaCl (500 ppm) and a flux of 28.6 L m^{-2} h^{-1} at 0.7 MPa, approaching the performance of a high-flux commercial RO membrane (DOW FILMTEC XLE).[197] The use of nanofiber membrane substrates can obviously replace fibrous cellulose substrates. In another study, interfacial polymerization was performed on CNF nanopaper using PEI and TMC to reduce the mean pore size of the membrane. The final pore size was less than 1 nm, making the resulting membrane suitable for NF application. The membrane was positively charged and displayed high permeation flux (32.68 L m^{-2} h^{-1} bar^{-1}) with decent rejection ratios against $MgSO_4$, $MgCl_2$, NaCl, and Na_2SO_4 (i.e., 65.3%, 89.7%, 43.6%, and 39.1%, respectively).[131] There are more examples of the incorporation of nanocellulose in the barrier layer for RO/NF applications that will not be discussed. We have summarized the use of nanocellulose as the matrix or the filler in the barrier layer of composite membranes in **Table 4**, along with their filtration applications, performance, and experimental conditions.

6.3. Environmental, Health, and Safety Considerations of Nanocellulose

Even though nanocellulose is extracted from biomass, there are always concerns regarding the use of nanocellulose from the perspectives of environmental, health, and safety considerations. Generally, nanocellulose (e.g., NCC and CNC) has a low toxicity profile, as first documented in 2010.[202] An overview of the literature[98,203] seems to suggest that any potential toxicity is associated with certain forms of nanocellulose, particularly after chemical modification. Most research studies have focused on the inhalation toxicology in terms of occupational exposure routes, as a result of the historically known hazards associated with nanoscale fibers and particles (e.g., asbestos). This is certainly also the case for cellulose nanoparticles, which have been shown to be cytotoxic, along with other constituents of wood such as saw dust.[204] For drinking water applications, we consider nanocellulose membranes to be reasonably safe. This is because many forms of nanocellulose have already been used in the food industry (e.g., food or processing additives) and have been proven to be safe. However, more studies are necessary to gain further insight into this subject.

6.4. Gravity-Driven Nanocellulose Membrane Filtration for Off-Grid Communities

We argue that nanocellulose, extracted from locally available and underutilized biomass sources (wood and nonwood plants) using cost-effective and environmentally friendly methods (e.g., the nitro-oxidation method), can be extremely useful to deal with various global drinking water challenges in off-grid communities, especially in underdeveloped countries. These materials can be used as absorbents, coagulants, and membranes. For adsorbents, nanocellulose may have effectiveness comparable with activated carbon materials for water purification. Activated carbon materials are usually derived from dense biomass sources (e.g., coconut shell, wood), but it may be more economically beneficial for nanocellulose adsorbents to be derived from loose biomass sources (e.g., agricultural residue).[205] There are many ways to use nanocellulose adsorbents in water purification; one possible method is the gravity-driven slow sand filtration method,[84,206] where one functional component is nanocellulose, which can remove small charged contaminants (e.g., fluoride and arsenic ions).

In the case of membrane filtration, we envision that the most eco-efficient method to remove a wide range of contaminants is by microfiltration that can be driven by gravity, where the membrane also possesses adsorption capability. One experimental setup was designed by a startup company called Liquidity Nanotech,[207] where the device can simultaneously remove bacteria, smaller viruses, and even toxic metal ions using gravity alone (**Figure 15**). Of course, with the low-cost production method to extract nanocellulose, many different forms of water purification techniques combining adsorption, coagulation, and membrane filtration functions using only cellulosic and nanocellulosic materials can be explored. These methods will truly help the poorest communities using their locally available materials and sustainable technologies to provide safe drinking water.

7. Concluding Remarks

During recent decades, it has become clear that nanotechnology and nanomaterials can play an important role in many water

Figure 15. An experimental gravity-driven microfiltration unit with membrane (in the pleated format) having both filtration and adsorption capabilities.

Table 4. Nanocellulose used as a barrier layer in composite membranes.

Barrier layer style	Substrate	Thickness of barrier layer	Pore size	Test conditions: Feed solution Pressure Time	Rejection [%]/flux/permeability/log reduction value (LRV)	Membrane	
Microcrystalline CNFs infused into PAN	PAN/PET	40–100 µm	>100 nm	0.2 µm particles (100 ppm)	98.2%	MF	[20]
Chemically modified CNFs infused into PAN	PAN/PET	40–100 µm	>100 nm	0.2 µm particles (100 ppm)	99.99%	MF	[20]
TEMPO-cellulose nanowhiskers infused into electrospun PAN	PAN/PET	–	0.22 µm	Pure water 0.2 µm particles *E. coli* 19.3 kPa	192 L m^{-2} h^{-1} 97.7% LRV = 6	MF	[17]
TEMPO-CNF	PAN/PET	0.10 ± 0.20 µm	54.6 nm	Water Oil/water 1350 ppm 30 psi, 48 h	500 L m^{-2} h^{-1} >99.6%	UF	[16]
TEMPO-Chitin	PAN/PET	0.10 ± 0.20 µm	–	Water	217 L m^{-2} h^{-1}	UF	[16]
TEMPO-NCC	PAN/PET	0.10 ± 0.20 µm	–	Water	272 L m^{-2} h^{-1}	UF	[16]
PVA and TEMPO-CNF	PAN/PET	0.85 ± 0.15 µm	6.1 nm	Oil/water 1350 ppm 30 psi, 24 h	400 L m^{-2} h^{-1} >99.5%	UF	[107]
CNF	PAN/PET	0.6 ± 0.1 µm	25 nm	Oil/water 1350 ppm 30 psi, 24 h	490 L m^{-2} h^{-1} 99.6%	UF	[185]
Chitin nanofiber	PAN/PET	0.6 ± 0.1 µm	27 nm	Oil/water 1350 ppm 30 psi, 24 h	239 L m^{-2} h^{-1} 99.6%	UF	[185]
Blend of nanocellulose–nanofiber and chitin–nanofiber	PAN/PET	0.6 ± 0.1 µm	14 nm	Oil/water 1350 ppm 30 psi, 100 h	250 L m^{-2} h^{-1} 99.5%	UF	[185]
Cellulose solution in ionic liquid cast on PAN layer	PAN/PET	0.3 µm	50 nm	Pure water Oil/water (1350 ppm) Dextran (2000 kDa) 30 psi 24 h	73.7 L m^{-2} h^{-1} 250 L m^{-2} h^{-1} 99.5% >90%	UF	[151]
Cellulose solution in urea/NaOH coated on electrospun cellulose acetate membrane	CA	40	–	Pure water Latex beads = 100 nm 10 kPa	89.47 L m^{-2} h^{-1} 99%	UF	[192]
TEMPO-CNF cross-linked using citric acid	Cellulose filter paper	–	23 µm	Oil/hexane (50:50 v/v) Gravity filtration	89.6 L m^{-2} h^{-1}	UF	[198]
NCC	PET-*co*-PVA		0.78–0.22 µm	Pure water Oil/water 0.25 MPa	378 L m^{-2} h^{-1} 99.6%	UF	[199]
2,3-Dicarboxy CNFs cross-linked using $CaCl_2$	PVDF	0.85 µm	10–55 nm	Pure water	72 kg/m^{-2} h^{-1} bar	UF	[153]
2,3-Dicarboxy CNFs cross-linked using $Na_3P_3O_9$	PVDF	0.85 µm	55 nm	Pure water	67 kg/m^{-2} h^{-1} bar	UF	[153]
TEMPO-CNF grafted with polyvinyl amine	PET/PAN		0.73 µm	Pure water Virus (MS2) Cr (VI) and Pb(II)	1300 L m^{-2} h^{-1} psi LRV = 4 100 mg g^{-1} 260 mg g^{-1}	UF	[200]
2,3-Dicarboxy CNFs	PVDF	0.85	–	Pure water Dextran (35–45 kDa)	175 kg/m^{-2} h^{-1} bar 74–80%	MF	[193]

Table 4. Continued.

Barrier layer style	Substrate	Thickness of barrier layer	Pore size	Test conditions: Feed solution Pressure Time	Rejection [%]/flux/permeability/log reduction value (LRV)	Membrane	
TEMPO CNF spray coated	PET/PAN	200 ± 20		Pure water Dextran (2000 kDa) 10 psi	69 L m^{-2} h^{-1} psi 75%	UF	[197]
TEMPO CNF followed by interfacial polymerization using PIP and TEA	PET/PAN	30 nm	0.3 nm	Pure water 2000 ppm $MgSO_4$ 482 kPa	2.2 L m^{-2} h^{-1} kPa >99% 44.7 L m^2 h^{-1}	NF	[152]
CNF impregnated into PVDF membrane	PVDF	–	–	Dye	2.9 mg g^{-1}	NF	[43]
Meldrum acid-modified CNF impregnated into PVDF	PVDF	–	–	Dye Fe_2O_3 NP's (20–100 nm)	3.9 mg g^{-1} >99%		[43]
TEMPO-CNF	Cellulose filter paper	–	2.4 nm	Water	47 L m^{-2} h^{-1} MPa	NF	[132]
CNF Phase inversion method	PES		70.9 nm	Water BSA 0.1 MPA 25 °C	813.3 L m^{-2} h^{-1} 91–95%	UF	[201]

remediation technologies. This article provides our perspective: that nanocellulose can be an important, safe, and economically sensible new nanomaterial that is particularly suitable for membrane applications. The nanocellulose-enabled membrane technologies have already been demonstrated in a few publications, and more will emerge in the near future. More importantly, these technologies can offer not only effective and cost-efficient platforms to advance large-scale water treatment processes for developed countries, but also may provide sustainable solutions to deal with many off-grid drinking water challenges in underdeveloped countries.

In this article, we discuss the fact that the existing large-scale commercial nanocellulose production technologies are primarily based on wood-based biomass. Although they have many advantages in terms of logistics and capacity for mass production, the use of cheaper processes and underutilized nonwood biomass, such as agricultural residues, for smaller-scale production may be particularly useful for developing countries. The article covers both the existing industrial manufacture of nanocellulosic materials from wood as well as new developments associated with low-cost nanocellulose extraction from nonwood plants, which are still in the initial stages. In addition, essential membrane properties, such as membrane strength (dry and wet), membrane pore size and porosity, long-term stability in aqueous media, as well as the membrane formats for different filtration applications (microfiltration, ultrafiltration, nanofiltration, and reverse osmosis), are discussed. These formats include self-standing membranes, thin film nanofibrous composite (TFNC) membranes, and nanocomposite barrier layers on varying scaffolds.

Acknowledgements

The authors acknowledge financial support from the Polymer Program of the Division of Materials Research in the National Science Foundation (DMR-1808690).

Conflict of Interest

The authors declare no conflict of interest.

Keywords

membrane, nanocellulose, water purification

Received: October 23, 2019
Revised: December 21, 2019
Published online: February 19, 2020

[1] WHO/UNICEF, https://www.unicef.org/publications/index_19033.html (accessed: August 2018).
[2] WHO/UNICEF, https://www.unicef.org/publications/index_82419.html (accessed: August 2018)
[3] A. Fenwick, *Science* **2006**, *313*, 1077.
[4] H. Voisin, L. Bergstrom, P. Liu, A. P. Mathew, *Nanomaterials* **2017**, *7*, 57.
[5] D. M. Warsinger, S. Chakraborty, E. W. Tow, M. H. Plumlee, C. Bellona, S. Loutatidou, L. Karimi, A. M. Mikelonis, A. Achilli, A. Ghassemi, L. P. Padhye, S. A. Snyder, S. Curcio, C. Vecitis, H. S. Arafat, J. H. Lienhard, *Prog. Polym. Sci.* **2016**, *81*, 209.

[6] M. P. del Pino, D. Bruce, *Desalination* **1999**, *124*, 271.
[7] B. Van der Bruggen, C. Vandecasteele, *Environ. Pollut.* **2003**, *122*, 435.
[8] G. Metreveli, L. Wågberg, E. Emmoth, S. Belák, M. Strömme, A. Mihranyan, *Adv. Healthcare Mater.* **2014**, *3*, 1546.
[9] A. Quellmalz, A. Mihranyan, *ACS Biomater. Sci. Eng.* **2015**, *1*, 271.
[10] M. Asper, T. Hanrieder, A. Quellmalz, A. Mihranyan, *Biologicals* **2015**, *43*, 452.
[11] a) B. Van Der Bruggen, C. Vandecasteele, T. Van Gestel, W. Doyen, R. Leysen, *Environ. Prog.* **2003**, *22*, 46; b) G. M. Geise, H. S. Lee, D. J. Miller, B. D. Freeman, J. E. McGrath, D. R. Paul, *J. Polym. Sci., Part B: Polym. Phys.* **2010**, *48*, 1685.
[12] a) B. S. Laila, V. Kochkodan, R. Hashaikeh, N. Hilal, *Desalination* **2013**, *326*, 77; b) H. Susanto, M. Ulbricht, *J. Membr. Sci.* **2009**, *327*, 125.
[13] G. R. Guillen, Y. Pan, M. Li, E. M. V. Hoek, *Ind. Eng. Chem. Res.* **2011**, *50*, 3798.
[14] J. E. Cadotte, M. Minn, *US Patent 4277344A*, **1981**.
[15] H. Ma, C. Burger, B. S. Hsiao, B. Chu, *J. Mater. Chem.* **2011**, *21*, 7507.
[16] H. Ma, C. Burger, B. S. Hsiao, B. Chu, *Biomacromolecules* **2011**, *12*, 970.
[17] H. Ma, C. Burger, B. S. Hsiao, B. Chu, *Biomacromolecules* **2012**, *13*, 180.
[18] Z. Khatri, G. Mayakrishnan, Y. Hirata, K. Wei, I. S. Kim, *Carbohydr. Polym.* **2013**, *91*, 434.
[19] Z. Wang, H. Ma, B. S. Benjamin, B. Chu, *Polymer* **2014**, *55*, 366.
[20] A. Sato, R. Wang, H. Ma, B. S. Hsiao, B. Chu, *J. Electron Microsc.* **2011**, *60*, 201.
[21] H. Ma, B. S. Hsiao, B. Chu, *ACS Macro Lett.* **2012**, *1*, 213.
[22] K. Medlock, https://inhabitat.com/6-ways-to-purify-water-without-expensive-technology/ (accessed: August 2018).
[23] R. Paul, https://inhabitat.com/6-water-purifying-devices-for-clean-drinking-water-in-the-developing-world/ (accessed: August 2018).
[24] https://designtoimprovelife.dk/donate-lifestraw-to-haiti/ (accessed: August 2018).
[25] https://www.lifestraw.com/stories/ecuador/ (accessed: August 2018).
[26] Tech Inspirations Ecoblue, http://causetech.net/innovation-zone/tech-inspirations/ecoloblue (accessed: August 2018).
[27] C. Mainhart, http://innovatedevelopment.org/2015/06/07/clay-pots-water-filters-easy-to-use-and-cheap-to-produce (accessed: August 2018).
[28] B. Meinhold, https://inhabitat.com/eliodomestico-solar-terra-cotta-water-filter-distills-5-liters-of-water-a-day/ (accessed: August 2018).
[29] Tech Inspirations Cycloclean, http://causetech.net/innovation-zone/tech-inspirations/cycloclean (accessed: August 2018).
[30] J. Heimbusch, https://www.treehugger.com/clean-technology/solar-powered-hamster-ball-purifies-water-for-drinking.html (accessed: August 2018).
[31] Tech Inspirations Life Sack, http://causetech.net/innovation-zone/tech-inspirations/life-sack (accessed: August 2018).
[32] a) C. S. Lee, J. Robinson, M. F. Chong, *Process Saf. Environ. Prot.* **2014**, *92*, 489; b) A. K. Verma, R. R. Dash, P. Bhunia, *J. Environ. Manage.* **2012**, *93*, 154; c) C. Y. Teh, P. M. Budiman, K. P. Y. Shak, T. Y. Wu, *Ind. Eng. Chem. Res.* **2016**, *55*, 4363; d) D. P. Zagklis, P. G. Koutsoukos, C. A. Paraskeva, *Ind. Eng. Chem. Res.* **2012**, *51*, 15456.
[33] a) C. S. Lee, M. F. Chong, J. Robinson, E. Binner, *Ind. Eng. Chem. Res.* **2014**, *53*, 18357; b) L. W. Zhang, J. R. Hua, W. J. Zhu, L. Liu, X. L. Du, R. J. Meng, J. M. Yao, *ACS Sustainable Chem. Eng.* **2018**, *6*, 1592; c) T. Suopajärvi, H. Liimatainen, O. Hormi, J. Niinimäki, *Chem. Eng. J.* **2013**, *231*, 59; d) T. Suopajärvi, E. Koivuranta, H. Liimatainen, J. Niinimäki, *J. Environ. Chem. Eng.* **2014**, *2*, 2005.
[34] A. Mautner, K. Y. Lee, T. Tammelin, A. P. Mathew, A. J. Nedoma, K. Li, A. Bismarck, *React. Funct. Polym.* **2015**, *86*, 209.
[35] R. Sahadevan, S. Schneiderman, C. Crandall, H. Fong, T. J. Menkhaus, *ACS Appl. Mater. Interfaces* **2017**, *9*, 41055.
[36] M. Hakalahti, A. Mautner, L. S. Johansson, T. Hänninen, H. Setälä, E. Kontturi, A. Bismarck, T. Tammelin, *ACS Appl. Mater. Interfaces* **2016**, *8*, 2923.
[37] A. Razaq, G. Nystrom, M. Stromme, A. Mihranyan, L. Nyholm, *PLoS One* **2011**, *6*, e29243.
[38] N. Ferraz, A. Leschinskaya, F. Toomadj, B. Fellström, M. Strømme, A. Mihranyan, *Cellulose* **2013**, *20*, 2959.
[39] a) D. Shi, F. Wang, T. Lan, Y. Zhang, Z. Shao, *Cellulose* **2016**, *23*, 1899; b) T. A. Dankovich, J. A. Smith, *Water Res.* **2014**, *63*, 245.
[40] K. Bethke, S. Palantöken, V. Andrei, M. Roß, V. S. Raghuwanshi, F. Kettemann, K. Greis, T. T. K. Ingber, J. B. Stückrath, S. Valiyaveettil, K. Rademann, *Adv. Funct. Mater.* **2018**, *28*, 1800409.
[41] T. Niu, J. Xu, W. Xiao, J. Huang, *RSC Adv.* **2014**, *4*, 4901.
[42] H. Fukuzumi, S. Fujisawa, T. Saito, A. Isogai, *Biomacromolecules* **2013**, *14*, 1705.
[43] D. A. Gopakumar, D. Pasquini, M. A. Henrique, L. C. de Morais, Y. Grohens, S. Thomas, *ACS Sustainable Chem. Eng.* **2017**, *5*, 2026.
[44] H. Sehaqui, B. Michen, E. Marty, L. Schaufelberger, T. Zimmermann, *ACS Sustainable Chem. Eng.* **2016**, *4*, 4582.
[45] Z. Karim, M. Hakalahti, T. Tammelin, A. P. Mathew, *RSC Adv.* **2017**, *7*, 5232.
[46] Z. Karim, A. P. Mathew, M. Grahn, J. Mouzon, K. Oksman, *Carbohydr. Polym.* **2014**, *112*, 668.
[47] Z. Karim, S. Claudpierre, M. Grahn, K. Oksman, A. P. Mathew, *J. Membr. Sci.* **2016**, *514*, 418.
[48] N. Mahfoudhi, S. Boufi, *Cellulose* **2017**, *24*, 1171.
[49] A. Dufresne, *Mater. Today* **2013**, *16*, 220.
[50] A. D. French, N. R. Bertoniere, R. M. Brown, H. Chanzy, D. Gray, K. Hattori, W. Glasser, in *Kirk–Othmer Encyclopedia of Chemical Technology*, 5th ed., Vol. *5* (Ed: R. Siedel), John Wiley & Sons, New York **2004**, p. 473.
[51] T. A. Boden, G. Marland, R. J. Andres, *Global, Regional and National Fossil-Fuel Carbon Dioxide Emissions*, US Department of Enrgy, Oak Ridge, TN **2010**.
[52] R. H. Atalla, in *Comprehensive Natural Products Chemistry* (Ed: B. M. Pinto), Elsevier, New York **1999**.
[53] a) C. Yao, F. Wang, Z. Cai, X. Wang, RSC Adv. **2016**, 6, 92648; b) M. Ali, M. Saleem, Z. Khan, I. A. Watson, in *Biomass, Biopolymer-Based Materials, and Bioenergy* (Eds: D. Verma, E. Fortunati, S. Jain, X. Zhang), Woodhead Publishing, UK/USA **2019**, p. 369; c) E. Iye, P. Bilsborrow, *Energy Policy* **2013**, *63*, 207.
[54] S. Boufi, in *Cellulose-Reinforced Nanofibre Composites*, (Eds: M. Jawaid, S. Boufi, A. Khalil H. P. S.), Woodhead Publishing, UK/USA **2017**, p. 129.
[55] T. Ahmed, B. Ahmad, *Pak. Dev. Rev.* **2014**, *53*, 275.
[56] a) N. S. Bentsen, C. Felby, B. J. Thorsen, *Prog. Energy Combust. Sci.* **2014**, *40*, 59; b) V. Menon, M. Rao, *Prog. Energy Combust. Sci.* **2012**, *38*, 522; c) M. Danish, M. Naqvi, U. Farooq, S. Naqvi, *Energy Procedia* **2015**, *75*, 2974; d) Y. Sun, J. Cheng, *Bioresour. Technol.* **2002**, *83*, 1; e) T. Shahzadi, S. Mehmood, M. Irshad, Z. Anwar, A. Afroz, N. Zeeshan, U. Rashid, K. Sughra, *Adv. Biosci. Biotechnol.* **2014**, *5*, 6; f) P. Kumar, D. M. Barrett, M. J. Delwiche, P. Stroeve, *Ind. Eng. Chem. Res.* **2009**, *48*, 3713.
[57] R. M. Brown Jr., I. M. Saxena, *Plant Physiol. Biochem.* **2000**, *38*, 57.
[58] S. Bardage, L. Donaldson, C. Tokoh, G. Daniel, *Nord. Pulp Pap. Res. J.* **2004**, *19*, 448.
[59] D. Klemm, F. Kramer, S. Moritz, T. Lindström, M. Ankerfors, D. Gray, A. Dorris, *Angew. Chem., Int. Ed.* **2011**, *50*, 5438.
[60] D. Klemm, E. D. Cranston, D. Fischer, M. Gama, S. A. Kedzior, D. Kralisch, F. Kramer, T. Kondo, T. Lindström, S. Nietzsche, K. Petzold-Welcke, F. Rauchfuß, *Mater. Today* **2018**, *21*, 720.

[61] a) P. R. Sharma, A. J. Varma, *Chem. Commun.* **2013**, *49*, 8818; b) P. R. Sharma, P. R. Rajamohanan, A. J. Varma, *Carbohydr. Polym.* **2014**, *113*, 615; c) P. R. Sharma, A. J. Varma, *Carbohydr. Polym.* **2014**, *114*, 339; d) P. R. Sharma, A. J. Varma, *Carbohydr. Polym.* **2014**, *104*, 135; e) P. R. Sharma, S. Kamble, D. Sarkar, A. Anand, A. J. Varma, *Int. J. Biol. Macromol.* **2016**, *87*, 460; f) A. J. Varma, P. R. Sharma, D. Sarkar, *US Patent 10017583B2*, **2010**.
[62] J. George, S. N. Sabapathi, *Nanotechnol., Sci. Appl.* **2015**, *8*, 45.
[63] G. Sebe, F. Ham-Pichavant, E. Ibarboure, A. L. Koffi, P. Tingaut, *Biomacromolecules* **2012**, *13*, 570.
[64] Y. Habibi, L. A. Lucia, O. J. Rojas, *Chem. Rev.* **2010**, *110*, 3479.
[65] R. J. Moon, A. Martini, J. Nairn, J. Simonsen, J. Youngblood, *Chem. Soc. Rev.* **2011**, *401*, 3941.
[66] A. Isogai, T. Saito, H. Fukuzumi, *Nanoscale* **2011**, *3*, 71.
[67] T. Lindström, J. Tulonen, P. Kolseth, *Holzforschung* **1987**, *41*, 225.
[68] S. Belbekhouche, J. Bras, G. Siqueira, C. Chappey, L. Lebrun, B. Khelifi, S. Marais, A. Dufresne, *Carbohydr. Polym.* **2011**, *83*, 1740.
[69] a) H. P. Abdul Khalil, Y. Davoudpour, M. N. Islam, A. Mustapha, K. Sudesh, R. Dungani, M. Jawaid, *Carbohydr. Polym.* **2014**, *99*, 649; b) T. Lindström, C. Aulin, A. Naderi, M. Ankerfors, in *Encyclopedia of Polymer Science and Technology*, John Wiley & Sons, New York **2014**.
[70] a) F. W. Herrick, R. L. Casebier, J. K. Hamilton, K. R. Sandberg, *J. Appl. Polym. Sci.: Appl. Polym. Symp.* **1983**, *37*, 797; b) A. F. Turbak, F. W. Snyder, K. R. Sandberg, *J. Appl. Polym. Sci.: Appl. Polym. Symp.* **1983**, *37*, 815.
[71] a) D. Page, presented at Trans. Symp. on Fundamentals of Papermaking Fibres, Cambridge, **1989**; b) K. Abe, S. Iwamoto, H. Yano, *Biomacromolecules* **2007**, *8*, 3276.
[72] M. Pääkkö, M. Ankerfors, H. Kosonen, A. Nykänen, S. Ahola, M. Österberg, J. Ruokolainen, J. Laine, P. T. Larsson, O. Ikkala, T. Lindström, *Biomacromolecules* **2007**, *8*, 1934.
[73] M. Henriksson, G. Henriksson, L. A. Berglund, T. Lindström, *Eur. Polym. J.* **2007**, *43*, 3434.
[74] T. T. T. Ho, T. Zimmermann, R. Hauert, W. Caseri, *Cellulose* **2011**, *18*, 1391.
[75] H. P. S. Abdul Khalil, A. H. Bhat, A. F. Ireana Yusra, *Carbohydr. Polym.* **2012**, *87*, 963.
[76] Y. Teramoto, N. Tanaka, S. H. Lee, T. Endo, *Biotechnol. Bioeng.* **2008**, *99*, 75.
[77] H. P. Zhao, X. Q. Feng, H. Gao, *Appl. Phys. Lett.* **2007**, *90*, 073112.
[78] T. Kondo, R. Kose, H. Naito, W. Kasai, *Carbohydr. Polym.* **2014**, *112*, 284.
[79] K. Uetani, H. Yano, *Biomacromolecules* **2011**, *12*, 348.
[80] A. Tejado, M. A. M. N. Alam, H. Yang, T. G. M. van de Ven, *Cellulose* **2012**, *19*, 831.
[81] H. Liimatainen, M. Visanko, J. A. Sirviö, O. O. Hormi, J. Niinimäki, *Cellulose* **2013**, *20*, 741.
[82] A. Olszewska, P. Eronen, L. Sisko-Johansson, J. M. Malho, M. Ankerfors, T. Lindström, J. Ruokalainen, J. Laine, M. Österberg, *Cellulose* **2011**, *18*, 1213.
[83] a) P. R. Sharma, A. Chattopadhyay, C. Zhan, S. K. Sharma, L. Geng, B. S. Hsiao, *Cellulose* **2018**, *25*, 1961; b) P. R. Sharma, A. Chattopadhyay, S. K. Sharma, B. S. Hsiao, *Ind. Eng. Chem. Res.* **2017**, *56*, 13885.
[84] P. R. Sharma, A. Chattopadhyay, S. K. Sharma, L. Geng, N. Amiralian, D. Martin, B. S. Hsiao, *ACS Sustainable Chem. Eng.* **2018**, *6*, 3279.
[85] a) P. R. Sharma, R. Joshi, S. K. Sharma, B. S. Hsiao, *Biomacromolecules* **2017**, *18*, 2333; b) P. R. Sharma, B. Zheng, S. K. Sharma, C. Zhan, R. Wang, S. R. Bhatia, B. S. Hsiao, *ACS Appl. Nano Mater.* **2018**, *1*, 3969.
[86] M. Ghanadpour, F. Carosio, P. T. Larsson, L. Wågberg, *Biomacromolecules* **2015**, *16*, 3390.
[87] T. Lindström, *Curr. Opin. Colloid Interface Sci.* **2017**, *29*, 68.
[88] R. J. Kerekes, C. J. Schell, *J. Pulp Pap. Sci.* **1992**, *18*, J32.
[89] A. Tejado, M. N. Alam, M. Antal, H. Yang, T. G. M. van de Ven, *Cellulose* **2012**, *19*, 831.
[90] a) E. Horvath, T. Lindström, *J. Colloid Interface Sci.* **2007**, *309*, 511; b) S. Zauscher, D. J. Klingenberg, *Colloids Surf. A* **2001**, *178*, 213.
[91] N. Amiralian, P. K. Annamalai, P. Memmott, E. Taran, S. Schmidt, D. J. Martin, *RSC Adv.* **2015**, *5*, 32124.
[92] a) S. Sharma, Y. Deng, *Ind. Eng. Chem. Res.* **2016**, *55*, 11467; b) B. S. Hsiao, B. Chu, P. R. Sharma, *US Patent 20180086851A1*, **2018**.
[93] S. E. Jacobsen, C. E. Wyman, *Appl. Biochem. Biotechnol.* **2000**, *84*, 81.
[94] D. I. Brink, *Tappi* **1961**, *44*, 256.
[95] a) D. I. Brink, *Tappi* **1961**, *44*, 263; b) D. I. Brink, *Tappi* **1962**, *45*, 315.
[96] a) S. A. Rydholm, *Pulping Processes*, Interscience Publishers, New York **1965**; b) T. P. Nevell, in *Oxidation of Cellulose New York*, (Eds: T. P. Nevell, S. H. Zeronian), Ellis Horwood Limited, Chichester, UK **1985**; c) F. N. Kaputskii, E. V. Gert, V. I. Torgashov, M. V. Shishonok, O. V. Zubets, *Chemical Problems of the Development of New Materials and Technologies*, (Eds: O. A. Ivashkevich, G. A. Branitsky, G. Y. Kabo, F. N. Kaputskii, L. P. Krul, A. I. Kulak, A. I. Lesnikovich, Yu. V. Nechepurenko, S. K. Rakhmanov) BSU, Russian **2003**, p. 264; d) E. V. Gert, V. I. Torgashov, O. V. Zubets, F. N. Kaputskii, *Cellulose* **2005**, *12*, 517.
[97] a) E. C. Yackel, W. O. Kenyon, *J. Am. Chem. Soc.* **1942**, *64*, 121; b) C. C. Unruh, W. O. Kenyon, *J. Am. Chem. Soc.* **1942**, *64*, 127.
[98] E. J. Foster, R. J. Moon, U. P. Agarwal, M. J. Bortner, J. Bras, S. Camarero-Espinosa, K. J. Chan, M. J. D. Clift, E. D. Cranston, S. J. Eichhorn, D. M. Fox, W. Y. Hamad, L. Heux, B. Jean, M. Korey, W. Nieh, K. J. Ong, M. S. Reid, S. Renneckar, R. Roberts, J. A. Shatkin, J. Simonsen, K. Stinson-Bagby, N. Wanasekara, J. Youngblood, *Chem. Soc. Rev.* **2018**, *47*, 2609.
[99] H. Fukuzumi, T. Saito, A. Isogai, *Carbohydr. Polym.* **2013**, *93*, 172.
[100] a) A. B. Fall, S. B. Lindström, O. Sundman, L. Ödberg, L. Wågberg, *Langmuir* **2011**, *27*, 11332; b) A. Naderi, T. Lindström, *Cellulose* **2015**, *22*, 1147.
[101] S. Iwamoto, W. Kai, T. Isogai, T. Saito, A. Isogai, T. Iwata, *Polym. Degrad. Stab.* **2010**, *95*, 1394.
[102] a) R. Das, M. D. Ali, S. B. A. Hamid, S. Ramakrishna, Z. Z. Chowdhury, *Desalination* **2014**, *336*, 97; b) J. H. Walther, K. Ritos, E. R. Cruz-Chu, C. M. Megaridis, P. Koumoutsakos, *Nano Lett.* **2013**, *13*, 1910.
[103] a) X. Qu, P. J. J. Alvarez, Q. Li, *Water Res.* **2013**, *47*, 3931; b) Md H. O. Rashid, S. F. Ralph, *Nanomaterials* **2017**, *7*, 99; c) R. Das, S. B. Abd Hamid, Md E. Ali, A. F. Ismail, M. S. M. Annuar, S. Ramakrishna, *Desalination* **2014**, *354*, 160; d) Ihsanullah, *Sep. Purif. Technol.* **2019**, *209*, 307; e) R. Das, *Carbon Nanotubes for Clean Water*, Springer International Publishing, Switzerland AG **2018**; f) D. A. Farahani, M. Hossein, V. Vahid, in *Nanoscale Materials in Water Purification* (Eds: S. Thomas, D. Pasquini, S. Y. Leu, D. A. Gopakumar), Elsevier, Amsterdam **2019**, p. 87.
[104] G. Ghasemzadeh, M. Momenpour, F. Omidi, M. R. Hosseini, M. Ahani, A. Barzegari, *Front. Environ. Sci. Eng.* **2014**, *8*, 471.
[105] Z. Wang, H. Ma, B. Chu, B. S. Hsiao, *J. Appl. Polym. Sci.: Appl. Polym. Symp.* **2017**, *134*, 44583.
[106] H. Ma, C. Burger, B. S. Hsiao, B. Chu, *ACS Macro Lett.* **2012**, *1*, 723.
[107] H. Ma, K. Yoon, L. X. Rong, M. Shokralla, A. Kopot, X. Wang, D. F. Fang, B. S. Hsiao, B. Chu, *Ind. Eng. Chem. Res.* **2010**, *49*, 11978.

[108] P. Cruz-Tato, E. O. Ortiz-Quiles, K. Vega-Figueroa, L. Santiago-Martoral, M. Flynn, L. M. Diaz-Vazquez, E. Nicolau, *Environ. Sci. Technol.* **2017**, *51*, 4585.
[109] M. E. Leitch, C. Li, O. Ikkala, M. S. Mauter, G. V. Lowry, *Environ. Sci. Technol. Lett.* **2016**, *3*, 85.
[110] N. Ferraz, D. O. Carlsson, J. Hong, R. Larsson, B. Fellström, L. Nyholm, M. Strømme, A. Mihranyan, *J. R. Soc., Interface* **2012**, *9*, 1943.
[111] a) Y. Nishi, M. Uryu, S. Yamanaka, N. Watanabe, N. Kitamura, M. Iguchi, S. Mitsuhashi, *J. Mater. Sci.* **1990**, *25*, 2997; b) S. Yamanaka, K. Watanabe, N. Kitamura, M. Iguchi, S. Mitsuhashi, Y. Nishi, M. Uryu, *J. Mater. Sci.* **1989**, *24*, 3141.
[112] T. Saito, Y. Nishiyama, J. L. Putaux, M. Vignon, A. Isogai, *Biomacromolecules* **2006**, *7*, 1687.
[113] a) A. Dufresne, *Nanocellulose: From Nature to High Performance Materials*, Walter de Gruyter, Berlin/Boston **2013**; b) A. Dufresne, *Curr. Opin. Colloid Interface Sci.* **2017**, *29*, 1.
[114] A. J. Benítez, A. Walther, *J. Mater. Chem. A* **2017**, *5*, 16003.
[115] a) S. Favier, R. Dendievel, G. Canova, Y. Cavaille, P. Gilormini, *Acta Mater.* **1997**, *45*, 1557; b) S. Favier, G. Canova, S. C. Schrivastava, J. Y. Cavaille, *Polym. Eng. Sci.* **1997**, *37*, 1732.
[116] a) T. Saito, R. Kuramae, J. Wohlert, L. A. Berglund, A. Isogai, *Biomacromolecules* **2013**, *14*, 248; b) S. Iwamoto, W. Kai, A. Isogai, T. Iwata, *Biomacromolecules* **2009**, *10*, 2571.
[117] R. Hori, M. Wada, *Cellulose* **2005**, *12*, 479.
[118] J. Huang, H. Zhu, Y. Chen, C. Preston, K. Rohrbach, J. Cumings, L. Hu, *ACS Nano* **2013**, *7*, 2106.
[119] a) J. Wang, D. J. Gardner, N. M. Stark, D. W. Bousfield, M. Tajvidi, Z. Cai, *ACS Sustainable Chem. Eng.* **2018**, *6*, 49; b) K. Chi, J. M. Catchmark, in *Green Polymer Chemistry: New Products, Processes, and Applications*, (Eds: H. H. Cheng, R. A. Gross, P. B. Smith) Vol. *1310*, American Chemical Society, Washington, DC **2018**, p. 109.
[120] Q. Wu, Y. Meng, K. Concha, S. Wang, Y. Li, L. Ma, S. Fu, *Ind. Crops Prod.* **2013**, *48*, 28.
[121] a) S. R. Djafari Petroudy, E. Rasooly Garmaroody, H. Rudi, *Carbohydr. Polym.* **2017**, *157*, 1883; b) K. Syverud, P. Stenius, *Cellulose* **2009**, *16*, 75.
[122] M. Henriksson, L. A. Berglund, P. Isaksson, T. Lindström, T. Nishino, *Biomacromolecules* **2008**, *9*, 1579.
[123] S. Gustafsson, A. Mihranyan, *ACS Appl. Mater. Interfaces* **2016**, *8*, 13759.
[124] H. Sehaqui, Q. Zhou, O. Ikkala, L. A. Berglund, *Biomacromolecules* **2011**, *12*, 3638.
[125] P. Orsolini, T. Marchesi D'Alvise, C. Boi, T. Geiger, W. R. Caseri, T. Zimmermann, *ACS Appl. Mater. Interfaces* **2016**, *8*, 33943.
[126] a) I. Mohmood, C. Batista Lopes, I. Lopes, I. Ahmad, C. Duarte, E. Pereira, *Environ. Sci. Pollut. Res.* **2013**, *20*, 1239; b) J. R. Werber, C. O. Osuji, M. Elimelech, *Nat. Rev. Mater.* **2016**, *1*, 16018; c) I. Gehrke, A. Geiser, A. Somborn-Schulz, *Nanotechnol., Sci. Appl.* **2015**, *8*, 1.
[127] a) A. W. Carpenter, C. F. de Lannoy, M. R. Wiesner, *Environ. Sci. Technol.* **2015**, *49*, 5277; b) N. Mohammed, N. Grishkewich, K. C. Tam, *Environ. Sci.: Nano* **2018**, *5*, 623;
[128] D. Qin, D. Zhang, Z. Shao, J. Wang, K. Mu, Y. liu, L. Zhao, *RSC Adv.* **2016**, *6*, 76336.
[129] C. Ao, W. Yuan, J. Zhao, X. He, X. Zhang, Q. Li, T. Xia, W. Zhang, C. Lu, *Carbohydr. Polym.* **2017**, *175*, 216.
[130] Q. G. Zhang, C. Deng, F. Soyekwo, Q. L. Liu, A. M. Zhu, *Adv. Funct. Mater.* **2016**, *26*, 792.
[131] F. Soyekwo, Q. Zhang, R. Gao, Y. Qu, C. Lin, X. Huang, A. Zhu, Q. Liu, *J. Membr. Sci.* **2017**, *524*, 174.
[132] A. Mautner, K. Y. Lee, P. Lahtinen, M. Hakalahti, T. Tammelin, K. Li, A. Bismarck, *Chem. Commun.* **2014**, *50*, 5778.
[133] D. A. Gopakumar, V. Arumughan, D. Pasquini, S.-Y. Leu, A. K. H.P.S, S. Thomas, in *Nanoscale Materials in Water Purification* (Eds: S. Thomas, D. Pasquini, S.-Y. Leu, D. A. Gopakumar), Elsevier, Amsterdam **2019**, p. 59.
[134] A. Dufresne, in *Nanocellulose: From Nature to High Performance Tailored Materials* (Ed: A. Dufresne), Walter de Gruyter, Berlin/Boston **2012**, p. 43.
[135] F. Ansari, L. A. Berglund, in *Multifunctional Polymeric Nanocomposites Based on Cellulosic Reinforcements* (Eds: D. Puglia, E. Fortunati, J. M. Kenny), William Andrew Publishing, Oxford/UK and Cambridge USA **2016**, p. 115.
[136] a) S. M. Alatalo, E. Mäkilä, E. Repo, M. Heinonen, J. Salonen, E. Kukk, M. Sillanpää, M. M. Titirici, *Green Chem.* **2016**, *18*, 1137; b) S. J. Chun, S. Y. Lee, G. H. Doh, S. Lee, J. H. Kim, *J. Ind. Eng. Chem.* **2011**, *17*, 521.
[137] Q. Li, W. Chen, Y. Li, X. Guo, S. Song, Q. Wang, Y. Liu, J. Li, H. Yu, J. Zeng, *Cellulose* **2016**, *23*, 1375.
[138] D. H. Page, *Tappi* **1969**, *52*, 674.
[139] T. Lindström, C. Fellers, M. Ankerfors, G. Glad-Nordmark, *Nord. Pulp Pap. Res. J.* **2016**, *31*, 459.
[140] A. J. Benitez, A. Walther, *Biomacromolecules* **2017**, *18*, 1642.
[141] C. Hagiopol, J. W Johnston, *Chemistry of Modern Papermaking*, CRC Press, Boca Raton, FL **2012**.
[142] A. J. Benitez, J. Torres-Rendon, M. Poutanen, A. Walther, *Biomacromolecules* **2013**, *14*, 4497.
[143] N. Chen, S. Hu, R. Pelton, *Ind. Eng. Chem. Res.* **2002**, *41*, 5366.
[144] a) H. H. Espy, *Tappi* **1995**, *78*, 90; b) S. A. Fischer, *Tappi* **1996**, *79*, 179.
[145] W. Yang, H. Bian, L. Jiao, W. Wu, Y. Deng, H. Dai, *RSC Adv.* **2017**, *7*, 31567.
[146] a) M. S. Toivonen, S. Kurki-Suonio, F. H. Schacher, S. Hietala, O. J. Rojas, O. Ikkala, *Biomacromolecules* **2015**, *16*, 1062; b) H. Zhang, L. Shi, X. Feng, *J. Mater. Chem. C* **2018**, *6*, 242.
[147] Y. Qing, R. Sabo, Z. Cai, Y. Wu, *Cellulose* **2013**, *20*, 303.
[148] F. Martoïa, P. J. J. Dumont, L. Orgéas, M. N. Belgacem, J. L. Putaux, *RSC Adv.* **2016**, *6*, 47258.
[149] A. Mautner, J. Lucenius, M. Österberg, A. Bismarck, *Cellulose* **2017**, *24*, 1759.
[150] T. Lindström, L. Wågberg, T. Larsson, presented at Trans. 13th Fundamental Res. Symp. on Advances in Paper Science and Technology, Cambridge, September **2005**.
[151] H. Ma, K. Yoon, L. X. Rong, Y. M. Mao, Z. R. Mo, D. F. Fang, Z. Hollander, J. Gaiteri, B. S. Hsiao, B. Chu, *J. Mater. Chem.* **2010**, *20*, 4692.
[152] X. Wang, D. Fang, B. S. Hsiao, B. Chu, *J. Membr. Sci.* **2014**, *469*, 188.
[153] M. Visanko, H. Liimatainen, J. A. Sirviö, O. Hormi, *Sep. Purif. Technol.* **2015**, *154*, 44.
[154] M. Visanko, H. Liimatainen, J. A. Sirviö, J. P. Heiskanen, J. Niinimäki, O. Hormi, *Biomacromolecules* **2014**, *15*, 2769.
[155] N. Pahimanolis, A. Salminen, P. A. Penttilä, J. T. Korhonen, L. S. Johansson, J. Ruokolainen, R. Serimaa, J. Seppälä, *Cellulose* **2013**, *20*, 1459.
[156] H. Orelma, M. Vuoriluoto, L. S. Johansson, J. M. Campbell, I. Filpponen, M. Biesalsky, O. J. Rojas, *RSC Adv.* **2016**, *6*, 85100.
[157] G. Dormán, G. D. Prestwich, *Biochemistry* **1994**, *33*, 5661.
[158] S. Kim, Y. Song, S. Ibsen, S. Y. Ko, M. J. Heller, *Carbon* **2016**, *109*, 624.
[159] a) H. Dong, J. F. Snyder, K. S. Williams, J. W. Andzelm, *Biomacromolecules* **2013**, *14*, 3338; b) L. Jowkarderis, T. G. M. van de Ven, *Cellulose* **2014**, *21*, 2511; c) R. Balamurugan, S. Sundarrajan, S. Ramakrishna, *Membranes* **2011**, *1*, 232.
[160] M. Shimizu, T. Saito, A. Isogai, *J. Membr. Sci.* **2016**, *500*, 1.
[161] Q. Meng, T. J. Wang, *Appl. Mech. Rev.* **2019**, *71*, 040801.

[162] a) J. M. B. Fernandes Diniz, M. H. Gil, J. A. A. M. Castro, *Wood Sci. Technol.* **2004**, *37*, 489; b) A. Idstrom, H. Brelid, M. Nyden, L. Nordstierna, *Carbohydr. Polym.* **2013**, *92*, 881; c) R. H. Newman, *Cellulose* **2004**, *11*, 45.
[163] M. Osterberg, J. Vartiainen, J. Lucenius, U. Hippi, J. Seppala, R. Serimaa, J. Laine, *ACS Appl. Mater. Interfaces* **2013**, *5*, 4640.
[164] M. Smyth, C. Fournier, C. Driemeier, C. Picart, E. J. Foster, J. Bras, *Biomacromolecules* **2017**, *18*, 2034.
[165] C. Baez, J. Considine, R. Rowlands, *Cellulose* **2014**, *21*, 347.
[166] A. Zerrouati, M. Rueff, B. Bouchekima, *Drying Technol.* **2015**, *33*, 1170.
[167] C. T. J. Dodson, W. W. Sampson, *J. Pulp Pap. Sci.* **1996**, *23*, J165.
[168] a) Y. Su, C. Burger, B. S. Hsiao, B. Chu, *J. Appl. Crystallogr.* **2014**, *47*, 788; b) Y. Mao, K. Liu, C. Zhan, L. Geng, B. Chu, B. S. Hsiao, *J. Phys. Chem. B* **2017**, *121*, 1340.
[169] W. Zhang, *Ph.D. Thesis*, Louisiana State University and Agricultural and Mechanical College, **2006**.
[170] H. Zhu, S. Zhu, Z. Jia, S. Parvinian, Y. Li, O. Vaaland, L. Hu, T. Li, *Proc. Natl. Acad. Sci. USA* **2015**, *112*, 8971.
[171] W. D. Campbell, *Tappi* **1959**, *42*, 999.
[172] L. R. Fisher, J. N. Israelachvili, *J. Colloid Interface Sci.* **1981**, *80*, 528.
[173] H. Fukuzumi, T. Saito, S. Iwamoto, Y. Kumamoto, T. Ohdaira, R. Suzuki, A. Isogai, *Biomacromolecules* **2011**, *12*, 4057.
[174] C. Aulin, M. Gällstedt, T. Lindström, *Cellulose* **2010**, *17*, 559.
[175] C. A. Bishop, in *Vacuum Deposition onto Webs, Films and Foils*, 2nd ed., **2011**, p. 197.
[176] W. Guo, H. H. Ngo, J. Li, *Bioresour. Technol.* **2012**, *122*, 27.
[177] M. A. Sirvain, M. Dalex, *Filtr. Sep.* **2015**, *52*, 14.
[178] R. Singh, in *Membrane Technology and Engineering for Water Purification*, 2nd ed., ScienceDirect, Elsevier, Amsterdam **2015**, p. 1.
[179] H. Sehaqui, Q. Zhou, L. A. Berglund, *Compos. Sci. Technol.* **2011**, *71*, 1593.
[180] T. Zimmermann, E. Pöhler, T. Geiger, *Adv. Eng. Mater.* **2004**, *6*, 754.
[181] H. Sehaqui, A. Liu, Q. Zhou, L. A. Berglund, *Biomacromolecules* **2010**, *11*, 2195.
[182] M. Nogi, S. Iwamoto, A. N. Nakagaito, H. Yano, *Adv. Mater.* **2009**, *21*, 1595.
[183] C. C. Aulin, T. Lindström, in *Biopolymers—New Materials for Sustainable Films and Coatings* (Ed: D. Plackett), John Wiley & Sons, Chichester, UK **2011**.
[184] H. Ma, C. Burger, B. S. Hsiao, B. Chu, *J. Membr. Sci.* **2014**, *454*, 272.
[185] H. Ma, B. S. Hsiao, B. Chu, *Polymer* **2011**, *52*, 2594.
[186] B. S. Lalia, E. Guillen, H. A. Arafat, R. Hashaikeh, *Desalination* **2014**, *332*, 134.
[187] C. Zhu, P. Liu, A. P. Mathew, *ACS Appl. Mater. Interfaces* **2017**, *9*, 21048.
[188] J. Zhou, Y.-L. Hsieh, *Nano Energy* **2020**, *68*, 104305.
[189] a) F. Jiang, H. Liu, Y. Li, Y. Kuang, X. Xu, C. Chen, H. Huang, C. Jia, X. Zhao, E. Hitz, Y. Zhou, R. Yang, L. Cui, L. Hu, *ACS Appl. Mater. Interfaces* **2018**, *10*, 1104; b) F. Jiang, T. Li, Y. Li, Y. Zhang, A. Gong, J. Dai, E. Hitz, W. Luo, L. Hu, *Adv. Mater.* **2018**, *30*, 1703453.
[190] C. Chen, Y. Li, J. Song, Z. Yang, Y. Kuang, E. Hitz, C. Jia, A. Gong, F. Jiang, J. Y. Zhu, B. Yang, J. Xie, L. Hu, *Adv. Mater.* **2017**, *29*, 1701756.
[191] a) B. Chu, B. S. Hsiao, H. Ma, *US Patent 2011/0198282 A1*, **2011**; b) B. Chu, B. S. Hsiao, H. Ma, *US Patent 2012/020206*, **2012**.
[192] W. Huang, Y. Wang, C. Chen, J. L. Law, M. Houghton, L. L. Chen, *Carbohydr. Polym.* **2016**, *143*, 9.
[193] M. Visanko, H. Liimatainen, J. A. Sirvio, A. Haapala, R. Sliz, J. Niinimaki, O. Hormi, *Carbohydr. Polym.* **2014**, *102*, 584.
[194] K. J. De France, T. Hoare, E. D. Cranston, *Chem. Mater.* **2017**, *29*, 4609.
[195] H. Liimatainen, M. Visanko, J. A. Sirvio, O. E. Hormi, J. Niinimaki, *Biomacromolecules* **2012**, *13*, 1592.
[196] H. Ma, B. S. Hsiao, in *Membrane Desalination Systems: The Next Generation* (Eds: A. Basile, E. Curcio, Inamuddin), Elsevier, Amsterdam **2018**, p. 81.
[197] X. Wang, H. Ma, B. Chu, B. S. Hsiao, *Desalination* **2017**, *420*, 91.
[198] K. Rohrbach, Y. Li, H. Zhu, Z. Liu, J. Dai, J. Andreasen, L. Hu, *Chem. Commun.* **2014**, *50*, 13296.
[199] D. Xu, X. Zheng, R. Xiao, *RSC Adv.* **2017**, *7*, 7108.
[200] R. Wang, S. Guan, A. Sato, X. Wang, Z. Wang, R. Yang, B. S. Hsiao, B. Chu, *J. Membr. Sci.* **2013**, *446*, 376.
[201] P. Qu, H. Tang, Y. Gao, L. P. Zhang, S. Wang, *BioResources* **2010**, *5*, 2323.
[202] T. Kovacs, V. Naish, B. O'Connor, C. Blaise, F. Gagné, L. Hall, V. Trudeau, P. Martel, *Nanotoxicology* **2010**, *4*, 255.
[203] a) C. Endes, S. Camarero-Espinosa, S. Mueller, E. J. Foster, A. Petri-Fink, B. Rothen-Rutishauser, C. Weder, M. J. D. Clift, *J. Nanobiotechnol.* **2016**, *14*, 78; b) G. M. DeLoid, I. S. Sohal, L. R. Lorente, R. M. Molina, G. Pyrgiotakis, A. Stevanovic, R. Zhang, D. J. McClements, N. K. Geitner, D. W. Bousfield, K. W. Ng, S. C. J. Loo, D. C. Bell, J. Brain, P. Demokritou, *ACS Nano* **2018**, *12*, 6469.
[204] M. J. D. Clift, E. J. Foster, D. Vanhecke, D. Studer, P. Wick, P. Gehr, B. Rothen-Rutishauser, C. Weder, *Biomacromolecules* **2011**, *12*, 3666.
[205] a) J. L. Huisman, G. Schouten, C. Schultz, *Hydrometallurgy* **2006**, *83*, 106; b) F. Fu, Q. Wang, *J. Environ. Manage.* **2011**, *92*, 407.
[206] a) P. R. Sharma, S. K. Sharma, R. Antoine, B. S. Hsiao, *ACS Sustainable Chem. Eng.* **2019**, *7*, 6140; b) https://phys.org/news/2014-12-nano-filter-environmentally-hazardous-industrial.html, 2014; c) L. Charerntanyarak, *Water Sci. Technol.* **1999**, *39*, 135.
[207] https://liquico.com/ (accessed: September 2019).

